HOMODYNE STUDIES OF LIGHT SCATTERED FROM A TURBULENT WATER JET

by

JOHN BARTON DeWOLF
A.B. Princeton University (1964)
S.M. Massachusetts Institute of Technology (1967)

SUBMITTED IN PARTIAL FULFILLMENT
OF THE REQUIREMENTS FOR THE
DEGREE OF DOCTOR OF
PHILOSOPHY
at the
MASSACHUSETTS INSTITUTE OF
TECHNOLOGY
June, 1969

Signature of Author .....
Department of
Earth and Planetary Sciences
May 16, 1969

Certified by .....
Thesis Supervisor

Accepted by .....
Chairman, Departmental Committee
on Graduate Students

WITHDRAWN
FROM
MIT LIBRARIES

ABSTRACT

HOMODYNE STUDIES OF LIGHT

SCATTERED FROM A TURBULENT WATER JET

by

JOHN BARTON DeWOLF

Submitted to the Department of Earth and Planetary Sciences
on May 21, 1969 in Partial Fulfillment of the
Requirement for the Degree of Doctor of Philosophy

It is found experimentally that the homodyne spectrum of coherent light scattered from particles suspended in a turbulent fluid is broader than the spectrum observed when the particles undergo Brownian motion in a fluid at rest. A theoretical and experimental study has been undertaken in order to relate the measured spectral widths and profiles to the parameters describing the turbulence. It is found theoretically that as long as the Lagrangian integral space scale is large compared to the wavelength, the homodyne spectrum has the same shape as the relative - velocity distribution. A simple Gaussian model is advanced for calculating spectral profiles numerically for the complicated situations which arise in practice. The experimental study involved scattering from uniform latex particles suspended in a turbulent water-into-water jet, and homodyne spectra were taken at different positions within the jet and for different Reynolds numbers. The variation of spectral width with position in the jet and with Reynolds number was as expected, but in cases where comparison with measurements on similar jets by other investigators was possible, the widths were systematically less than expected. Some possible explanations are offered.

Thesis Supervisor: Dr. Giorgio Fiocco

Former Title: Assistant Professor of Geophysics

At Present: Senior Scientist
European Space Research Institute
Frascati (Roma) Italy

When we try to pick out anything by itself, we find it hitched to everything else in the universe.

-John Muir

TABLE OF CONTENTS

		Page
I.	THE PROBLEM AND ITS CONTEXT	7
	1. Introduction	7
	2. Homodyne versus heterodyne spectroscopy	10
	3. Historical summary	12
	4. Overview of the thesis	14
II.	SPECTRUM OF THE SCATTERED LIGHT	15
	5. Introduction	15
	6. Autocorrelation and spectral density of the scattered electric field	19
	7. Autocorrelation and spectral density of the scattered intensity	28
	8. Particles undergoing Brownian motion	31
	9. Particles in turbulent motion	35
III.	EXPERIMENTAL STUDY OF A TURBULENT WATER JET	39
	10. Introduction	39
	11. Description of the apparatus	40
	12. Analysis of the printed data	51
	13. Observed spectrum for Brownian particles	53
	14. Observed spectrum as a function of Reynolds number and position in the jet	55
IV.	CONCLUSIONS	68
	15. Summary of results	68
	16. Suggestions for future experiments	69
APPENDIX I		71
	17. Autocorrelation and spectral density of a random process	71
APPENDIX II		75
	18. The anode photocurrent random process	75
	18.1 Mean value of the anode photocurrent	75
	18.2 Autocorrelation and spectral density of the anode photocurrent	78
APPENDIX III		82
	19. The scattered electric field	82
APPENDIX IV		86
	20. Space-time correlation of the scattered intensity and the area of coherence	86
APPENDIX V		94
	21. Signal-to-noise ratio for the homodyne spectrometer	94

	Page
LIST OF SYMBOLS	96
BIBLIOGRAPHY	99
BIOGRAPHICAL NOTE	103

LIST OF FIGURES AND PHOTOGRAPHS

		Page
1.	Geometry associated with the scattering region.	20
2.	Diagram of the hydraulics.	41
3.	Photograph of the jet, Re = 380.	43
4.	Photograph of the jet, Re = 630.	44
5.	Photograph of the jet, Re = 2530.	45
6.	Photograph of the jet, Re = 5055.	46
7.	Photograph of the apparatus.	48
8.	Diagram of the spectrometer.	49
9.	Spectrum of light scattered from 910Å diameter spheres undergoing Brownian motion in a water solution.	54
10.	Spectrum of light scattered from 910Å diameter spheres suspended in a turbulent water jet. Axial position = 80 ND; Re = 505.	56
11.	Spectrum of light scattered from 910Å diameter spheres suspended in a turbulent water jet. Axial position = 80 ND; Re = 2530.	57
12.	Width of the scattered spectrum as a function of jet nozzle Reynolds number.	58
13.	Spectrum of light scattered from 910Å diameter spheres suspended in a turbulent water jet. Axial position = 40 ND; Re = 505.	63
14.	Width of the scattered spectrum as a function of axial position in nozzle diameters.	64
15.	Width of the scattered spectrum as a function of radial position at selected axial positions.	65
16.	Theoretical width of the spectrum from a fully turbulent jet as a function of radial position.	66
17.	Geometry of the spatial correlation calculation.	90

ACKNOWLEDGMENTS

The author is deeply grateful to Dr. Giorgio Fiocco for his friendship, advice, assistance, and unfailing encouragement over the past five years. I am indebted to Dr. Fiocco for his many suggestions regarding the experimental program, for his assistance is taking and analyzing data, and for numerous helpful discussions concerning the theory of particle motions. I would like to express my sincere appreciation to Jacques Thompson for his assistance and advice on countless occasions, for his construction of several parts of the apparatus, and for his help in obtaining the excellent photographs of the jet. I am grateful to Dr. Theodore Madden and Dr. Charles Counselman for critically reading the manuscript and suggesting a number of improvements. I would also like to thank Dr. Thomas Greytak and Dr. George Benedek for several helpful discussions concerning the theory of the experiment. Finally, I would like to thank Dr. Gerald Grams for his good-humored assistance on many occasions, particularly with the computer programming.

The use of the facilities of the Research Laboratory of Electronics and of the Francis Bitter National Magnet Laboratory is gratefully acknowledged. This work was supported in part by the National Aeronautics and Space Administration under Grant NGR 22-009-131.

I. THE PROBLEM AND ITS CONTEXT

1. Introduction

An interesting optical technique has been developed recently for measuring molecular diffusion coefficients of monodisperse systems of small particles in fluid suspension (Cummins, Knable, and Yeh, 1964; Dubin, Lunacek, and Benedek, 1967). The technique is to measure the frequency spectrum of laser light (continuous wave) scattered from the particles with a device known as an optical homodyne spectrometer. The diffusion coefficient is determined directly by measuring the width of the spectrum. The technique requires some kind of low frequency spectrum analyzer (a wave analyzer works very well), but does not require any other elaborate electronic apparatus and places only modest requirements on the laser power.

It has been suggested (Frisch, 1967, and others) that similar spectral studies of light scattered from fluid turbulence might yield some useful information about velocity fluctuation distributions and correlations. The optical technique is particularly attractive because it can be used to investigate turbulence in liquids where hot wire anemometry is difficult, and because there are no mechanical probes involved which might disturb the flow. Several optical heterodyne studies of turbulent flow in pipes have already been reported (Pike, Jackson, Bourke, and Page, 1967; Goldstein and Hagen, 1967; Goldstein and Kreid, 1967), and the results suggest that the homodyne technique will work well and give useful information.

Development of the homodyne technique would be of geophysical interest for several reasons. A technique for the measurement of

turbulence parameters on a small scale in the atmosphere would be of use in micrometeorology, particularly for the measurement of the vertical component of fluctuation velocities. There is also a need for a technique to detect the presence of clear air turbulence at a distance. Since the homodyne spectrum is not frequency shifted by changes in the mean velocity (see below), homodyne as opposed to heterodyne detection may be advantageous for detecting the presence of turbulence in situations for which the mean velocity varies widely or is unknown. It may also be difficult to provide a reference signal for heterodyning in atmospheric experiments. Another geophysical application not related to turbulence concerns measurement of the molecular diffusion coefficient for various types of aerosol particles. It might be possible, for example, to determine particle size distributions for naturally occurring atmospheric aerosols by measuring the shape of the homodyne spectrum.

Some preliminary unsuccessful experiments were carried out by the author which involved homodyne detection of light scattered by aerosol-gaseous mixtures. Not enough light was scattered by naturally-occurring aerosols in our laboratory to allow a spectral measurement with the He-Ne laser available. An experiment with a steam jet had to be abandoned when it became evident that observed spectra were due to concentration fluctuations and not phase modulation. These experiments did yield some useful results concerning the ratio of aerosol-to-molecular scattered light when the scattered spectrum was observed interferometrically (see Fiocco and DeWolf, 1968).

We report here on the application of an optical homodyne spectrometer to the study of turbulence in liquids. We have observed the transition between diffusion-broadened spectra in the absence of turbulence

to spectra broadened by velocity fluctuations in a water-into-water jet. The variation of spectral width with position in the jet and with Reynolds number was as expected, but the actual widths measured were systematically less than expected on the basis of measurements due to other investigators on similar jets. The discrepancy is presumably due to differences between their jets and ours, and some possible explanations are offered in connection with the more detailed description of the experiment in Chapter III.

It is hoped that the results obtained in this experiment on liquids may be of some use in planning and interpreting experiments to be carried out later using aerosols to study atmospheric turbulence.

2. Homodyne versus heterodyne spectroscopy

The process of spectrum measurement and the distinction between homodyne and heterodyne spectroscopy may be understood by considering the following experiment.

A laser beam is scattered by small particles suspended in a fluid medium of low scattering power.* A portion of the scattered light is made to fall on the light-sensitive cathode of a photomultiplier. As the particles move about in the fluid, their individual scattered electric fields are each phase-modulated or Doppler shifted. The total scattered intensity fluctuates because "beats" occur between the frequencies of the individual scattered electric fields. The power spectrum of the intensity will contain these difference-frequencies which will generally be confined to a narrow band centered about zero frequency. Since the photocurrent is proportional to the intensity, the power spectrum of the photocurrent also contains these difference-frequencies. A spectral analysis of the fluctuating photocurrent therefore contains some information about the statistics of the particle velocities. By analogy with radio-frequency detectors, this device is known as the self-beat or homodyne spectrometer.

In the optical heterodyne spectrometer, the scattered light is mixed with a relatively intense portion of the unscattered light which corresponds to the local oscillator signal in a radio heterodyne. Beats (intermediate frequencies) are now generated between the frequencies of the individual scattered electric fields and the local oscillator frequency.

---

*Alternatively, the laser beam may be scattered by the fluid medium directly.

With this type of detection, one can also determine any non-zero average frequency difference between the scattered and unscattered light. This feature allows the heterodyne spectrometer to be used as a velocimeter for measuring mean flow velocities. The optical homodyne on the other hand is not sensitive to a mean flow velocity, but only to velocity differences. The width of the spectrum therefore will depend not only on the magnitude of the turbulent velocity fluctuations, but also on the spatial correlation of velocities in the scattering volume.

3. Historical summary

A few words may be in order about the development of the homodyne technique and some other uses to which it has been put.

Optical mixing spectroscopy dates from a remarkable experiment performed by Forrester, Gudmundsen, and Johnson (1955) using incoherent light. They were able to observe a beat signal between Zeeman components of the mercury green line by constructing a sensitive photodetector, modulating the signal relative to the noise, and by using very long integration times. The experiment helped to settle a certain controversy about optical coherence.

When laser sources became available, mixing experiments became relatively easy to perform and a number of applications were suggested including studies of laser mode structure and spectral line shapes (Forrester, 1961; but see Smith and Williams, 1962).

The first light scattering experiment using optical mixing for spectral analysis was that of Cummins, Knable, and Yeh (1964). They used a heterodyne detection scheme and scattered He-Ne laser light from a dilute solution of small, uniform polystyrene latex spheres to measure diffusion coefficients. Slightly modified versions of this apparatus were used to obtain spectra for scattering from concentration fluctuations in binary mixtures near the critical temperature (Alpert, Yeh, and Lipworth, 1965; Alpert, 1966).

The first light scattering experiments to use a homodyne detection scheme were those of Ford and Benedek (1965; 1966), who were able to measure spectra of light scattered from density fluctuations in a pure liquid near the critical point. They developed a simple version of the homodyne spectrometer which has been used in several subsequent

investigations, including the present. Other experiments were those of White, Osmundson, and Ahn (1966) who scattered from a critical solution of macromolecules, and Lastovka and Benedek (1966 A, B) who measured the spectrum of the central component of light scattered from a normal liquid.

Homodyne studies of the diffusion of macromolecules have been reported by Dubin, Lunacek, and Benedek (1967), Arecchi, Giglio, and Tartari (1967), and Dunning and Angus (1968). Diffusion coefficients for liquid-in-liquid solutions have recently been measured using the optical homodyne by Aref'ev, Kopylovskii, Mash, and Fabelinskii (1967). These experiments are described briefly in section 8 after the theory has been discussed.

4. Overview of the thesis

The body of the thesis is divided into two parts: one dealing with the spectrum of the scattered light from the theoretical point of view (Chapter II), the other dealing with experimental results obtained by scattering from a turbulent water jet (Chapter III).

In Chapter II, it was our intention to show how the homodyne spectrum can be related to the probability density function for the relative displacement of two particles. When the Lagrangian integral space scale (roughly, the average distance it takes a small fluid lump to change its velocity appreciably) is long compared to the wavelength of the light (more precisely, compared to the reciprocal of the magnitude of the difference vector $\vec{K}$), then the homodyne spectrum has the same shape as the relative velocity distribution for particles in the volume. This will depend in general on the size of the scattering volume relative to the length over which velocities are correlated.

In Chapter III, the width and shape of the homodyne spectrum observed as a function of position in the jet and jet Reynolds number are described. An attempt was made to compare widths calculated on the basis of a simple model with measured widths, but the results are somewhat inconclusive due to some uncertainties about the jet behavior.

Conclusions and suggestions for future experiments will be found in Chapter IV,

The reader's attention is called to the summary of definitions and formulas concerning the autocorrelation and spectral density of a random process which is presented in Appendix I.

A list of symbols with page references and the bibliography will be found at the end.

II. SPECTRUM OF THE SCATTERED LIGHT

5. Introduction

The object of this chapter is to relate the spectrum of coherent light scattered from a collection of small, randomly-located, moving particles to the statistics of the particle motion. A theoretical development is given which shows that the power spectral density of the intensity of the scattered light depends in general on the joint probability density function (p.d.f.) of particle displacements for two particles. This function is readily evaluated for particles undergoing Brownian motion. By introducing a number of simplifying assumptions, one can also calculate the function approximately in the more complicated case in which the particles are suspended in a turbulent fluid.

We are interested in the situation in which the scattered light is detected using a homodyne spectrometer. In the homodyne spectrometer, the spectrum of the light intensity incident on the surface of a photomultiplier is determined by measuring the spectrum of the anode photocurrent.* The relation between the spectrum of the anode photocurrent and the spectrum of the light intensity has been given by Freed and Haus (1966) and can be written (the low frequency approximation to the shot-noise spectrum is used)

---

*in this chapter, we consider only the case in which the photocathode is by assumption coherently illuminated, by which we mean illuminated such that a given intensity fluctuation occurs simultaneously over the entire cathode. Such a situation may be always realized in practice by placing a sufficiently small aperture in front of the cathode. A brief consideration of the more general spatial-temporal coherence problem for light scattering from a dilute suspension of particles having homogeneous statistics is given in Appendix IV, where an expression is found for the size of a naturally-occurring coherence area.

$$S_i(f) = G e \bar{i} + \left(\frac{\bar{i}}{\bar{I}}\right)^2 S_I(f) \quad , \qquad (1)$$

where $S_i(f)$ is the spectral power density of the photocurrent i, $S_I(f)$ is the spectral power density of the light intensity I, G is the current gain of the tube, e is the electronic charge, and $\bar{i}$ and $\bar{I}$ are the mean values of the photocurrent and the light intensity respectively. The photocurrent spectrum is seen to consist of a variable part due to fluctuations in the light intensity, and a constant, shot-noise part which is due to the discrete nature of the photoelectron pulses. A derivation of equation (1) will be found in Appendix II.

Previous authors have obtained an expression for the spectrum of the scattered intensity by first obtaining an expression for the electric field spectrum and then relating the two by assuming that the electric field is a Gaussian random variable (Ford and Benedek, 1966). The electric field spectrum is given by several authors (e.g., Komarov and Fisher, 1963); for incoherent scattering of a monochromatic plane wave from a statistically homogeneous collection of infinitesimal particles, it can be written

$$S_E(f) = \text{const.} \int d\tau \int d\vec{\rho}\; p(\vec{\rho}\,;\tau)\, \exp i\left[2\pi(f_o - f) - \vec{K}\cdot\vec{\rho}\right] \quad , \qquad (2)$$

where f_o is the incident frequency, $\vec{K} = \vec{k}_o - \vec{k}_s$ is the vector difference between incident and scattered wave vectors, and $p(\vec{\rho}\,;\tau)$ is the p.d.f. for the probability that a particle is displaced a distance $\vec{\rho}$ in the time interval τ .* If the electric field has Gaussian statistics to second order, then the intensity spectrum is given by

---

*Since we consider only incoherent scattering, the corresponding probability density function for distinct particles has been omitted.

$$S_I(f) = \bar{I}^2\,\delta(f) + \mathcal{C}^2 \int_{-\infty}^{\infty} df'\, S_E(f' + f)\, S_E(f') \quad , \tag{3}$$

where $\mathcal{C}$ is a constant. Once an expression has been found for $p(\vec{\rho}\,;\tau)$, then equations (2) and (3) constitute a solution to the theoretical problem.

When the scattering particles are suspended in a turbulent fluid however, it is no longer possible to assume that the electric field statistics are Gaussian to second order since, as will be shown, in order to derive equation (3) it is necessary to assume that particle motions are independent. Particle velocities in the turbulent flow will in general be spatially correlated because of the velocity correlations which exist in the fluid.

In section 7 of this chapter, we show that when particle statistics are homogeneous, the intensity spectrum is in general given by

$$S_I(f) = \bar{I}^2 \Big[\delta(f) + \int_{-\infty}^{\infty} d\tau \int d\vec{\Delta} \int d\vec{\rho}_1 \int d\vec{\rho}_2\; p(\vec{\rho}_1, \vec{\rho}_2, \vec{\Delta}; \tau)\, \exp i\left[\vec{K}\cdot(\vec{\rho}_1 - \vec{\rho}_2) - 2\pi f \tau\right] \Big] \quad , \tag{4}$$

where $p(\vec{\rho}_1, \vec{\rho}_2, \vec{\Delta}; \tau)$ is a joint p.d.f., $\vec{\rho}_1$ and $\vec{\rho}_2$ are the displacements in a time τ of particles 1 and 2 respectively, and $\vec{\Delta}$ is the separation of the particles at the initial instant.

Of great importance in determining the shape of the observed spectrum is the ratio of the Lagrangian integral space scale of the particle motions to the quantity $1 / |\vec{K}|$, as is shown in connection with a discussion of scattering from Brownian particles in section 8.

In most turbulent situations, the integral scale will be large compared with $1 / |\vec{K}|$, so that equation (4) neglecting molecular diffusion can be written directly in terms of the turbulent velocities

$$S_I(f) = \bar{I}^2 \left\{ \delta(f) + \int d\vec{\Delta} \int d\vec{v}_1 \int d\vec{v}_2 \; p(\vec{v}_1, \vec{v}_2, \vec{\Delta}) \delta\left[f - \frac{\vec{K} \cdot (\vec{v}_1 - \vec{v}_2)}{2\pi} \right] \right\}, \quad (5)$$

as will be shown in section 9. The spectrum in this case consists of beats between Doppler shifted frequencies scattered by the individual particles.

Although the experiment discussed in this paper can be interpreted in terms of equation (5), it should be pointed out that the general form in equation (4) might be of use in other situations. If experiments could be devised (at longer wavelengths, for example) in which the Lagrangian integral scale is comparable with (or smaller than) $1 / |\vec{K}|$, then information on the function $p(\vec{\rho}_1, \vec{\rho}_2, \vec{\Delta}; \tau)$ could be obtained using equation (4). This function is of considerable interest in the theory of turbulent diffusion. An interesting possibility would be to observe the spectrum as a function of scattering angle, thus making $1 / |\vec{K}|$ large or small with respect to the Lagrangian integral scale. These and other possibilities are readily visualized by use of the bivariate Gaussian model which is introduced in section 9 below.

We begin by considering in the next section, the steps which lead to equation (2) for the electric field spectrum.

6. Autocorrelation and spectral density of the scattered electric field

In this section we give a brief derivation of the expression for the (power) spectral density* of the scattered electric field. The procedure is to derive an expression for the electric field autocorrelation and then Fourier transform it to find the spectrum. The electric field is treated as an ergodic stationary random process, and the autocorrelation is found by ensemble averaging using the method discussed in Appendix I. After an expression for the spectral density is derived, two special cases are discussed for illustration.

The expressions discussed in this section can be found in several recent papers (Komarov and Fisher, 1963; Pecora, 1964; Fiocco and DeWolf, 1968). Our purpose in this section is to demonstrate both the method of derivation and the usefulness of this type of approach. The same method is used in the next section to find a similar expression for the scattered intensity.

An expression for the scattered electric field is derived in Appendix III. The associated geometry is shown in Fig. 1. The incident electric field $\vec{E}(\vec{r},t)$ is assumed to be a plane, monochromatic wave of the form

$$\vec{E}(\vec{r},t) = \vec{E}_o \exp i(\omega_o t - \vec{k}_o \cdot \vec{r}), \tag{6}$$

where

$$|\vec{k}_o| = \frac{\omega_o}{c},$$

*The terms "spectral density" and "spectrum" in this paper always refer to power spectral density, a quantity which is defined in Appendix I.

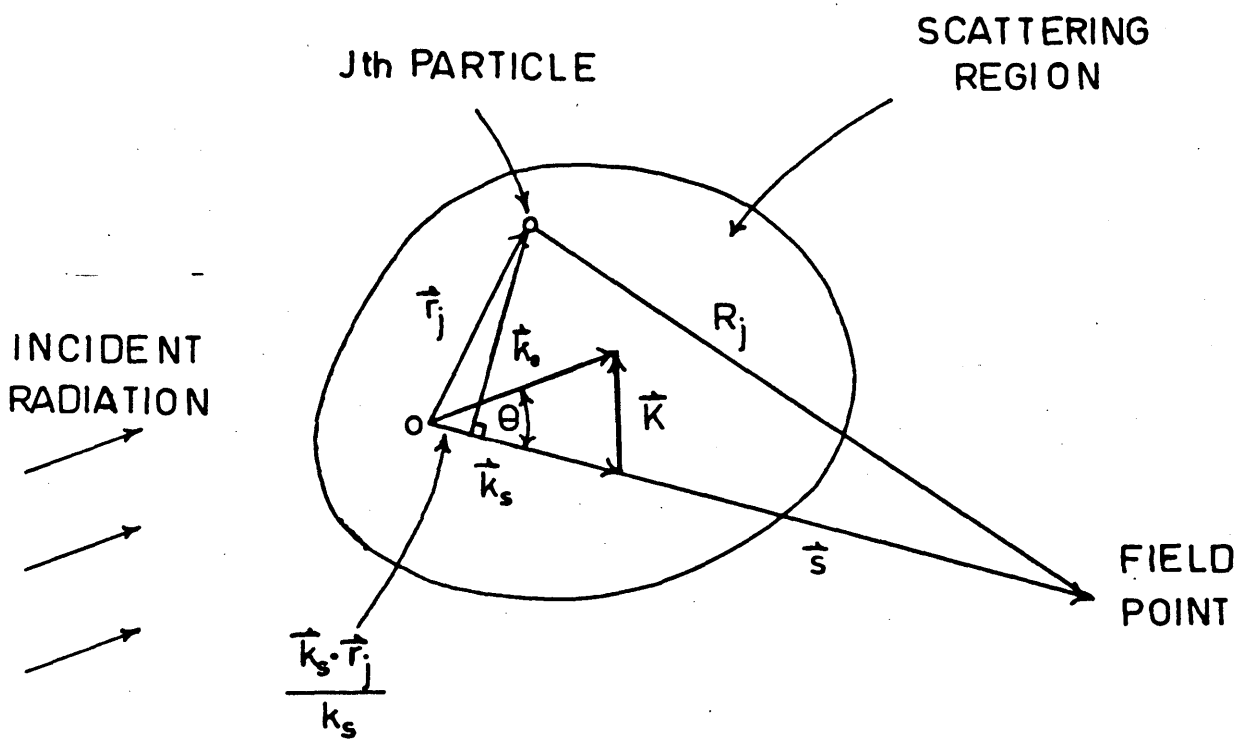

Fig. 1. Geometry associated with the scattering region.

and $\omega_o = 2\pi f_o$ is a real, constant angular frequency. The scattering particles are assumed to be point electric dipoles with velocities small compared to the velocity of light. Attenuation of the wave and multiple scattering are neglected. With these assumptions, the scattered electric field at a distance s large compared to the dimensions of the scattering volume was shown to be

$$\vec{E}(\vec{s},t) \simeq -\frac{q_o}{s} \exp i(\omega_o t - k_o s) \sum_{j=1}^{N} \exp\left[-i\vec{K}\cdot\vec{r}_j(t)\right], \tag{7}$$

where N is the total number of particles, $\vec{r}_j(t)$ is the location of the j^{th} particle, and

$$\vec{K} = \vec{k}_o - \vec{k}_s, \tag{8}$$

where $\vec{k}_s$ is a wave vector in the scattering direction. The constant q_o is given by

$$q_o = \alpha k_o^2 E_o \sin\Upsilon, \tag{9}$$

where α is the polarizability of the particle, and Υ is the angle between the incident electric field and the scattering direction.

It should be noted that

$$|\vec{K}| = \frac{4\pi}{\lambda_o} \sin\frac{\theta}{2}, \tag{10}$$

where λ_o is the incident wavelength ($\lambda_o = c/f_o$) and θ is the angle between the incident and scattered wavevectors.

In constructing the autocorrelation of the electric field using equation (7), we will assume that the scattering is incoherent for the sake of simplicity. The significance of this assumption is most readily seen when the mean value of the scattered intensity is calculated.

The scattered intensity $I(\vec{s}, t)$ (power crossing a unit area placed normal to the scattering direction) is by definition

$$I(\vec{s},t) = \mathcal{C}\, E(\vec{s},t)\, E^{*}(\vec{s},t), \tag{11}$$

where the asterisk denotes complex conjugate and

$$\mathcal{C} = \begin{cases} \frac{1}{2}\sqrt{\frac{\epsilon_o}{\mu_o}} & \text{m.k.s.} \\ \frac{c}{8\pi} & \text{Gaussian c.g.s.} \end{cases}$$

Using the above expression for $E(\vec{s},t)$ we find

$$I(\vec{s},t) = \frac{\mathcal{C} q_o^{\,2}}{s^2} \sum_{j=1}^{N} \sum_{k=1}^{N} \exp i\vec{K}\cdot\left[\vec{r}_k(t) - \vec{r}_j(t)\right]. \tag{12}$$

The intensity is defined as a real quantity and the complex exponentials could be replaced by cosines, but we choose to leave it in the above form to simplify later manipulations.

To find the mean value of the intensity, we divide the double summation in equation (12) into N terms for which j = k and $(N^2 - N)$ terms for which $j \neq k$. The result is

$$\bar{I} = \frac{\mathcal{C} q_o^{\,2}}{s^2}\left[N + \overline{\sum_{\substack{j=1 \\ j\neq k}}^{N} \sum_{k=1}^{N} \exp i\vec{K}\cdot\left[\vec{r}_k(t) - \vec{r}_j(t)\right]}\right]. \tag{13}$$

The mean intensity is seen to consist of two terms: the first term represents incoherent scattering; the second term takes into account diffraction by the scattering volume as a whole and coherent phase relationships which may exist between different particles.

The assumption that the scattering is incoherent implies that the second term in equation (13) is negligible; that is, that the phases scattered by different particles are independent and that diffraction may be neglected. The phases will be effectively independent if the concentration is dilute so that the particles are non-interacting. As long as the scattering volume is large compared to the wavelength, diffraction will be negligible except near the forward direction where $\vec{K}$ is small and the phase of the exponential doesn't vary much over the volume. In the

following discussion we neglect terms of this type.

For our purposes then

$$\bar{I} = \frac{\mathcal{C} q_o^2 N}{s^2} \,. \tag{14}$$

In the case of incoherent scattering, the mean value of the scattered intensity is just N times the intensity scattered by a single particle.

Essentially the same procedure is now used to find the autocorrelation of the electric field. Using equation (A9) as the definition of the complex autocorrelation and equation (7) for the electric field, we find

$$R_E(\tau) = \frac{q_o^2}{s^2} \exp(i\omega_o\tau) \left[\overline{\sum_{j=1}^{N} \exp i\vec{K}\cdot\left[\vec{r}_j(t_2) - \vec{r}_j(t_1)\right]} + \overline{\sum_{j=1}^{N} \sum_{\substack{k=1 \\ j\neq k}}^{N} \exp i\vec{K}\cdot\left[\vec{r}_k(t_2) - \vec{r}_j(t_1)\right]} \right], \tag{15}$$

where $\tau = t_1 - t_2$, and we have divided the terms in the double summation as was done for the intensity. As with the intensity, the summation over terms for which $j \neq k$ is assumed to be negligible. Since the particles are indistinguishable, the average of the first summation may be expressed as N times the average of a given term. Constructing the ensemble average as indicated in Appendix I, one has

$$R_E(\tau) = \frac{Nq_o^2}{s^2} \exp(i\omega_o\tau) \int_V d\vec{r}_1 \int_V d\vec{r}_2 \exp i\vec{K}\cdot\left[\vec{r}_2 - \vec{r}_1\right] p(\vec{r}_1, \vec{r}_2; \tau), \tag{16}$$

where $p(\vec{r}_1, \vec{r}_2; \tau)$ is the joint probability density that a given particle is located at $\vec{r}_1$ at time t_1 and at $\vec{r}_2$ at time $t_2 = t_1 - \tau$. The integrals are to be taken over the scattering volume V. This is the

general expression for the electric field autocorrelation when the scattering is incoherent.

When the particle statistics are homogeneous, the expression for the electric field autocorrelation may be simplified. In this case*

$$p(\vec{r}_1, \vec{r}_2; \tau) = p(\vec{r}_2 | \vec{r}_1; \tau) p(\vec{r}_1) = p(\vec{\rho}; \tau) \frac{1}{V} \quad , \tag{17}$$

where $\vec{\rho} = \vec{r}_1 - \vec{r}_2$. Thus $p(\vec{r}_1, \vec{r}_2; \tau)$ depends only upon the displacement $\vec{\rho}$ of the particle in the time τ, and not upon location in the volume. The autocorrelation becomes

$$R_E(\tau) = \frac{Nq_o^2}{s^2} \exp(i\omega_o \tau) \int_{V \otimes V} d\vec{\rho} \exp\left[-i \vec{K} \cdot \vec{\rho}\right] p(\vec{\rho}; \tau) \quad , \tag{18}$$

where the $d\vec{\rho}$ integration must be over a weighted volume which represents the convolution (designated $\otimes$) of V with itself.

The spectrum of the electric field may now be obtained by Fourier transforming the autocorrelation function with respect to τ (see equation (A11)). For the homogeneous case, one obtains

$$S_E(f) = \frac{Nq_o^2}{s^2} \int_{-\infty}^{\infty} d\tau \int_{V \otimes V} d\vec{\rho} \exp i\left[2\pi(f_o - f) - \vec{K} \cdot \vec{\rho}\right] p(\vec{\rho}; \tau) \quad . \tag{19}$$

Equation (17) is essentially the result given by Komarov and Fisher (1963) (their equation (24)) restricted to the case of incoherent scattering (our $p(\vec{\rho}; \tau)$ is the same as their $G_1(\vec{r}; \tau)$). When the scattering volume is large compared with the non-zero region of $p(\vec{\rho}; \tau)$, then the spectrum of the electric field is seen to be the space-time Fourier transform

---

*The notation $p(a|b)$ denotes a conditional probability density function; that is, the probability density of a, given b.

of the correlation $p(\vec{\rho}\,;\tau)$.*

The connection between equation (19) and the ordinary Doppler shift concept is readily seen. For if all the particles move with constant velocity $\vec{v}$, then

$$p(\vec{\rho}\,;\tau) = \delta(\vec{\rho} - \vec{v}\tau), \tag{20}$$

and the integrals may be carried out (see equations (A18) and (A19)) to obtain

$$S_E(f) = \frac{Nq_o^2}{s^2}\,\delta\left[(f_o - f) - \frac{\vec{K}\cdot\vec{v}}{2\pi}\right] . \tag{21}$$

More insight into the usefulness of equation (19) for light scattering problems can be obtained by considering two other slightly more complicated examples.

First consider the case in which the particles move with constant velocity but in which the velocities are distributed according to a Gaussian law (e.g., scattering from the molecules of a low density gas). The correlation function may be written

$$p(\vec{\rho}\,;\tau) = \int d\vec{v}\; p(\vec{\rho}\mid\vec{v}\,;\tau)\, p(\vec{v}) , \tag{22}$$

where $p(\vec{\rho}\mid\vec{v}\,;\tau)$ is the probability density that a particle travels a

---

*The functions $p(\vec{r}_2 \mid r_1;\tau)$ and the special case $p(\vec{\rho}\,;\tau)$ are functions of considerable importance in a number of statistical particle theories, notably Brownian motion, turbulent diffusion, and fluid statistical mechanics. In the latter connection, $p(\vec{\rho}\,;\tau)$ corresponds to the self-correlation part of the van Hove correlation function introduced by van Hove (1954) to describe neutron scattering from systems of interacting particles.

distance $\vec{\rho}$ in a time τ given that the initial velocity of the particle is $\vec{v}$. In the case postulated

$$p(\vec{\rho} \mid \vec{v}; \tau) = \delta(\vec{\rho} - \vec{v}\tau), \tag{23}$$

and

$$p(\vec{v}) = \left(\frac{3}{2\pi \overline{v^2}}\right)^{\frac{3}{2}} \exp\left[-\frac{3|\vec{v}|^2}{2\overline{v^2}}\right] . \tag{24}$$

On substituting into equation (22) one finds

$$p(\vec{\rho}; \tau) = \left(\frac{3}{2\pi \overline{v^2}\tau^2}\right)^{\frac{3}{2}} \exp\left[-\frac{3|\vec{\rho}|^2}{2\overline{v^2}\tau^2}\right] . \tag{25}$$

The expressions for the electric field autocorrelation and spectrum are

$$R_E(\tau) = \frac{Nq_o^2}{s^2} \exp(i\omega_o\tau) \exp\left[-\frac{K^2\overline{v^2}\tau^2}{6}\right] , \tag{26}$$

and

$$S_E(f) = \frac{Nq_o^2}{s^2}\left(\frac{6\pi}{K^2\overline{v^2}}\right)^{\frac{1}{2}} \exp\left[-\frac{6\pi^2(f_o - f)^2}{K^2\overline{v^2}}\right] . \tag{27}$$

The familiar expression for the spectrum of light scattered from a low density gas may be obtained by substituting for K^2 as given in equation (10) and recalling that $\overline{v^2} = 3k_BT/m$ where k_B is Boltzmann's constant, T is the temperature, and m is the mass of the particle.

The second example we consider is scattering from particles undergoing a random walk. If the particle suffers n displacements per unit time and the mean square length of a step is $\overline{l^2}$, then asymptotically as the number of steps becomes large (Chandrasekhar, 1943, p. 16)

$$p(\vec{\rho}\,;\,\tau) = \left[\frac{1}{4\pi D|\tau|}\right]^{\frac{3}{2}} \exp\left[-\frac{|\vec{\rho}|^2}{4\,D|\tau|}\right] \quad , \tag{28}$$

where

$$D = \frac{\overline{n\,l^2}}{6} \quad , \tag{29}$$

is a diffusion coefficient. This leads to the following expressions for the electric field autocorrelation and spectrum:

$$R_E(\tau) = \frac{q_o^2 N}{s^2} \exp(i\omega_o\tau) \exp(-K^2 D|\tau|), \tag{30}$$

and

$$S_E(f) = \frac{q_o^2 N}{s^2} \frac{1}{\pi} \frac{(K^2 D/2\pi)}{(f_o - f)^2 + (K^2 D/2\pi)^2} \quad . \tag{31}$$

The spectrum has a Lorentzian shape in this case with a half width at half maximum (HWHM) of $K^2D/2\pi$ hz. Although the Doppler shift concept is difficult to apply in this case, equation (19) formulated in terms of the correlation function $p(\vec{\rho}\,;\,\tau)$ gives the answer directly.

The interpretation of this result is most illuminating from the continuum point of view. In this view, the light is scattered by random fluctuations in the concentration of the particles caused by the random walk. These concentration fluctuations decay exponentially in time causing the spectrum of the electric field to have a Lorentzian shape. The function $p(\vec{\rho}\,;\,\tau)$ is sometimes referred to as a density correlation function.

7. Autocorrelation and spectral density of the scattered intensity

The spectral density of the scattered intensity can be calculated using the same assumptions and procedures that have been used in the previous section. As indicated in the introduction to this chapter, we are particularly interested in the case in which the particles do not move independently. That is, we want to allow for the possibility that particles may be carried along more or less en masse by the fluid.

The autocorrelation of the scattered intensity is found by substituting from equation (12) into the definition equation (A5) to find

$$R_I(\tau) = \frac{\mathcal{C}^2 q_o^4}{s^4} \overline{\sum_{j=1}^{N} \sum_{k=1}^{N} \sum_{\ell=1}^{N} \sum_{m=1}^{N} \exp i \vec{K} \cdot \left[\vec{r}_k(t_1) - \vec{r}_j(t_1) - \vec{r}_\ell(t_2) + \vec{r}_m(t_2) \right]} \quad . \tag{32}$$

Fortunately, this formidable expression has comparatively few non-negligible terms. In fact, the only terms which we need consider are those for which

$j = k = l = m$	N terms
$j = k;\ l = m;\ j \neq l$	$N^2 - N$ terms

and

$j = m;\ k = l;\ j \neq k$	$N^2 - N$ terms .

The other terms are negligible since they are of the same order of magnitude as the diffraction term in equation (13). Separating out the above terms we find for the autocorrelation

$$R_I(\tau) = \frac{\mathcal{C}^2 q_o^4}{s^4} \left[N + (N^2 - N) + \sum_{\substack{j=1 \\ j \neq k}}^{N} \sum_{k=1}^{N} \exp i \vec{K} \cdot \left[\vec{r}_j(t_2) - \vec{r}_j(t_1) - \vec{r}_k(t_2) + \vec{r}_k(t_1) \right] \right] \quad . \tag{33}$$

The averaging is carried out in the same manner as in the previous section. One finds (assuming N is large) that

$$R_I(\tau) = \bar{I}^2 \left[1 + \int\vec{dr}_{11}\int\vec{dr}_{12}\int\vec{dr}_{21}\int\vec{dr}_{22} \exp i\vec{K}\cdot\left[\vec{r}_{12}-\vec{r}_{11}-\vec{r}_{22}+\vec{r}_{21}\right] \right.$$

$$\left. \times p\left(\vec{r}_{11},\vec{r}_{12},\vec{r}_{21},\vec{r}_{22};\tau\right) \right] , \qquad (34)$$

where $\vec{r}_{jk}$ denotes the position of the j^{th} particle at time t_k. Equation (34) is the general expression for the intensity autocorrelation corresponding to equation (16).

This expression reduces to a familiar result if it is assumed that particle motions are independent. In that case

$$p(\vec{r}_{11}, \vec{r}_{12}, \vec{r}_{21}, \vec{r}_{22}; \tau) = p(\vec{r}_{11}, \vec{r}_{12}; \tau)\, p(\vec{r}_{21}, \vec{r}_{22}; \tau) , \qquad (35)$$

and one finds

$$R_I(\tau) = \bar{I}^2 + C^2 R_E(\tau)\, R_E^*(\tau) , \qquad (36)$$

where $R_E(\tau)$ is given by equation (16). This equation is equivalent to a result obtained by Lawson and Uhlenbeck (1950) (section 6.2, equation (8)) in connection with radar scattering from systems of random particles or clutter. Their result is of interest because they were able to derive first and second order probability densities for the electric field and the intensity. Both first and second order probability densities for the electric field are Gaussian as long as 1.) the number of scattering particles is large, and 2.) particle motions are independent. Equation (36) is recognizable as the autocorrelation of the output of a square-law device when the input is a complex Gaussian random process.

The spectrum for this case is easily found by application of the convolution theorem for Fourier transforms, equation (A17):

$$S_I(f) = \bar{I}^2\,\delta(f) + \mathcal{C}^2\int_{-\infty}^{\infty} df'\; S_E(f' + f)\; S_E(f') \quad . \tag{37}$$

These simple relations are no longer valid when particle motions are correlated. In that case one must consider the general function $p(\vec{r}_{11}, \vec{r}_{12}, \vec{r}_{21}, \vec{r}_{22}; \tau)$ displayed in equation (34).

Equation (34) may be simplified when the particle statistics are homogeneous. In that case

$$p(\vec{r}_{11}, \vec{r}_{12}, \vec{r}_{21}, \vec{r}_{22}; \tau) = p(\vec{r}_{22}, \vec{r}_{21}, \vec{r}_{12} \,|\, \vec{r}_{11}; \tau)\; p(\vec{r}_{11})$$
$$= p(\vec{\rho}_1, \vec{\rho}_2, \vec{\Delta}; \tau)\; \frac{1}{V} \quad ,$$

where $\vec{\rho}_1 = \vec{r}_{11} - \vec{r}_{12}$, $\vec{\rho}_2 = \vec{r}_{21} - \vec{r}_{22}$, are the displacements of particles 1 and 2 respectively, and $\vec{\Delta} = \vec{r}_{11} - \vec{r}_{21}$ is the separation of the particles at the initial time. The autocorrelation becomes

$$R_I(\tau) = \bar{I}^2 \left[1 + \int d\vec{\Delta} \int d\vec{\rho}_1 \int d\vec{\rho}_2\; p(\vec{\rho}_1, \vec{\rho}_2, \vec{\Delta}; \tau)\; \exp\left[i\,\vec{K}\cdot(\vec{\rho}_2 - \vec{\rho}_1)\right] \right] \quad , \tag{37A}$$

so that the expression for the spectrum is

$$S_I(f) = \bar{I}^2 \Bigg[\delta(f) + \int_{-\infty}^{\infty} d\tau \int d\vec{\Delta} \int d\vec{\rho}_1 \int d\vec{\rho}_2\; p(\vec{\rho}_1, \vec{\rho}_2, \vec{\Delta}; \tau)\; \exp i\left[\vec{K}\cdot(\vec{\rho}_1 - \vec{\rho}_2) - 2\pi f \tau\right] \Bigg] \quad , \tag{37B}$$

which is equation (4) of the introduction.

We will see in section 9 below that when it can be assumed that over distances long compared to $1 / |\vec{K}|$, the particle velocities are constant, the spectrum is determined by the distribution of <u>relative</u> velocities, as one might expect from elementary considerations. Before showing this, we consider the case of scattering from Brownian particles.

8. Particles undergoing Brownian motion

We now make use of the results obtained in the previous two sections to obtain an expression for the intensity spectrum of light scattered from Brownian particles. The particles are assumed to move independently so that equations (36) and (37) are applicable. We wish to show the importance of the ratio of the Lagrangian scale for the diffusion process to the reciprocal of the difference wave vector $\vec{K}$ in determining the shape of the observed spectrum.

The intensity spectrum for scattering from particles undergoing the special type of random walk mentioned in section 6 may be readily obtained by substituting from equation (31) into equation (37). We find

$$S_I(f) = \bar{I}^2 \left[\delta(f) + \frac{1}{\pi} \frac{(K^2D/\pi)}{f^2 + (K^2D/\pi)^2} \right], \tag{38}$$

which apart from the delta function is a Lorentzian curve having a HWHM of K^2D/π hz. This is the spectrum obtained when the individual steps of the walk become vanishingly small, since equation (28) for $p(\vec{\rho}\,;\tau)$ is asymptotically valid only in that limit.

It is not difficult to show that equation (38) is actually valid as long as the Lagrangian integral scale of the diffusion process is small compared to $1/|\vec{K}|$.

The general expression for $p(\vec{\rho}\,;\tau)$ for an Ornstein-Uhlenbeck type of random walk in which the particle velocities have a Gaussian distribution can be written (Chandrasekhar, (1943))

$$p(\vec{\rho}\,;\tau) = \left[\frac{3}{2\pi\,\overline{\rho^2}(\tau)} \right]^{3/2} \exp\left[-\frac{3\,|\vec{\rho}\,|^2}{2\,\overline{\rho^2}(\tau)} \right], \tag{39}$$

where

$$\overline{\rho^2}(\tau) = \frac{2\overline{v^2}}{B^2}\left[e^{-B|\tau|} + B|\tau| - 1\right] \quad , \tag{40}$$

in which B represents the friction constant. For spherical particles of radius a and mass m in a medium of viscosity η , B is given by

$$B = \frac{6\pi a\eta}{m} \quad .$$

Thus the p.d.f. for particle displacements is Gaussian with a time dependent variance $\overline{\rho^2}(\tau)$. By expanding the exponential in equation (55), one can show that when $|\tau|$ is small, $\overline{\rho^2}$ is proportional to τ^2. When $|\tau|$ is large however, $\overline{\rho^2}$ is proportional to τ , as would be expected for a diffusion process. Furthermore, by setting $D = \overline{v^2}/\,3B$ so that

$$D = \frac{k_B T}{6\pi a\eta} \quad , \tag{41}$$

one can show that equation (39) reduces to equation (28) for large τ.

The ratio $\sqrt{\overline{v^2}}/B$ is the Lagrangian length scale for the diffusion process (Hinze, 1959) which we designate Λ.

Substituting equation (39) into equation (18) one finds

$$R_E(\tau) = \frac{N q_0^2}{s^2}\exp(i\omega_0\tau)\exp\left[-\frac{K^2\Lambda^2}{3}\left(e^{-B|\tau|} + B|\tau| - 1\right)\right] \quad . \tag{42}$$

When $K^2\Lambda^2 \gg 1$, then $R_E(\tau)$ is negligible except for small τ in which case the spectrum has the Gaussian form given in equation (27). In general one must expand the second exponential to obtain (Pecora, 1964)

$$\exp\left[-\frac{K^2\Lambda^2}{3}\left(e^{-B|\tau|} + B|\tau| - 1\right)\right]$$

$$= \sum_{n=0}^{\infty} \frac{1}{n!}\left[-\frac{K^2\Lambda^2}{3}\right]^n \exp\left[-B\left(n + \frac{K^2\Lambda^2}{3}\right)|\tau|\right]\exp\left(\frac{K^2\Lambda^2}{3}\right) \quad ,$$

and then Fourier transform with respect to τ to obtain

$$S_E(f) = 2\frac{Nq_o^2}{s^2}\exp\left[\frac{K^2\Lambda^2}{3}\right]\sum_{n=0}^{\infty}\frac{1}{n!}\left[-\frac{K^2\Lambda^2}{3}\right]^n \frac{B\left[n+\frac{K^2\Lambda^2}{3}\right]}{4\pi^2(f_o-f)^2 + B^2\left[n+\frac{K^2\Lambda^2}{3}\right]^2} \quad (43)$$

When $K^2\Lambda^2 << 1$, terms beyond n = 0 in this expression are negligible and the electric field spectrum has the Lorentzian form given in equation (31).

Thus the shape of the spectrum depends critically on whether the integral scale Λ is large or small compared with $1 / |\vec{K}|$. For light scattering from small Brownian particles in a liquid, Λ is small compared to $1 / |\vec{K}|$, and the intensity spectrum should be given by equation (38).

This prediction has been investigated experimentally by several researchers.

The first experimental (heterodyne) observation of the spectrum of light scattered by Brownian particles was that of Cummins, Knable, and Yeh (1964). They used spherical polystyrene latex particles in a water solution and investigated angular dependence and particle size dependence of the scattered linewidths. The measured linewidths were larger than predicted, particularly for the larger particles (2a = 5500Å). They attributed the excess broadening to thermal convection currents in the medium.

Dubin, Lunacek, and Benedek (1967) investigated the spectra obtained from solutions of similar latex particles as well as solutions of various other biologically interesting macromolecules. The latex particles gave spectra which were accurately Lorentzian having widths in close agreement with the predicted values. Angular dependence and particle size dependence of the spectra were as expected. The largest latex particle

size measured was d = 3660Å. The more complicated macromolecules gave non-Lorentzian spectra.

Arecchi, Giglio, and Tartari (1967) found theory and experiment in agreement for the smaller latex particles, but for the d = 5500Å particles, the measured widths were again systematically too large.

Dunning and Angus (1968) reported good agreement with theory using latex spheres coated with a monolayer of soap to prevent agglomeration. They investigated the temperature dependence of the diffusion coefficient and reported some difficulty with convection currents at the higher temperatures. They also emphasized that care must be taken to prevent light scattered from stationary surfaces in the apparatus from reaching the photomultiplier.

Aref'ev, Kopylovskii, Mash, and Fabelinskii (1967) reported satisfactory results in measuring diffusion coefficients for liquid solutions of acetone in carbon disulfide, and bromoform in n-propanol.

One may conclude that the theory given in this section for scattering from Brownian particles seems to explain the observed spectra except that a residual broadening due to something like convection currents* is sometimes apparent and is particularly noticeable in the narrower spectra (due to the larger particles).

*Photophoresis may also be of importance here.

9. Particles in turbulent motion

In this section, we apply the results of section 7 above to the problem of scattering from particles in a turbulent fluid. In section 7, an equation was derived (equation (37B)) which expressed the intensity spectrum in terms of the function $p(\vec{\rho}_1, \vec{\rho}_2, \vec{\Delta}; \tau)$. If it is assumed that the Lagrangian integral scale for the turbulence is large compared with $1 / |\vec{K}|$ as it ordinarily would be at optical wavelengths, then the spectrum can be expressed directly in terms of the turbulent velocities, as we shall see.

We make the following additional assumptions. 1. It is assumed that the particles are passive, that is, that they do not have any influence on the flow or on each other. 2. It is assumed that the particle is of approximately the same density as the medium and that it is small compared to the scale of the smallest turbulent fluctuation. Under these circumstances, the particle will closely follow the fluid motion except for molecular diffusion (see Hinze, 1959, pp. 352-64). 3. Finally, it is assumed that the Brownian motion of a particle is independent of its motion due to turbulence so that the processes may be considered separately. The observed spectrum would then be a convolution of a spectrum due to Brownian motion (equation (38)) with a spectrum due to the turbulent velocities. This is probably a reasonable assumption as long as the turbulence does not create large density gradients in the fluid.

Let us suppose then that molecular diffusion is absent and that over a scale length $1 / |\vec{K}|$, turbulent velocities are constant though correlated and distributed according to some law.

The intensity spectrum can be expressed in terms of the velocities by a procedure similar to that used for the electric field spectrum (see

equations (22) and (23)). One can write

$$p(\vec{\rho}_1,\vec{\rho}_2,\vec{\Delta};\tau) = \int d\vec{v}_1 \int d\vec{v}_2 \; p(\vec{\rho}_1,\vec{\rho}_2|\vec{v}_1,\vec{v}_2,\vec{\Delta};\tau)\; p(\vec{v}_1,\vec{v}_2,\vec{\Delta}) \quad , \tag{44}$$

where $\vec{v}_1$ and $\vec{v}_2$ are the velocities of particles 1 and 2 respectively. According to the above assumptions

$$p(\vec{\rho}_1,\vec{\rho}_2|\vec{v}_1,\vec{v}_2,\vec{\Delta};\tau) = \delta(\vec{\rho}_1 - \vec{v}_1\tau)\,\delta(\vec{\rho}_2 - \vec{v}_2\tau) \quad . \tag{45}$$

When equations (44) and (45) are substituted into equation (37B) one obtains

$$S_I(f) = \bar{I}^2\left\{\delta(f) + \int_{-\infty}^{\infty} d\tau \int d\vec{\Delta} \int d\vec{v}_1 \int d\vec{v}_2 \; \exp i\left[\vec{K}\cdot(\vec{v}_1-\vec{v}_2) - 2\pi f\right]\tau \; p(\vec{v}_1,\vec{v}_2,\vec{\Delta})\right\} . \tag{46}$$

The integral over τ can be performed to give

$$S_I(f) = \bar{I}^2\left\{\delta(f) + \int d\vec{\Delta} \int d\vec{v}_1 \int d\vec{v}_2 \; \delta\left[f - \frac{\vec{K}\cdot(\vec{v}_1-\vec{v}_2)}{2\pi}\right] p(\vec{v}_1,\vec{v}_2,\vec{\Delta})\right\} \quad . \tag{47}$$

The spectrum is thus determined by the distribution of <u>relative</u> velocities in the volume.

Two limiting situations are of interest. First, if the scattering volume is small compared to the (Eulerian) velocity correlation scale, then the fluid velocity is essentially the same throughout the volume. The spectrum given by equation (47) is very narrow. Second, if the scattering volume is large compared to the velocity correlation scale, then most velocity pairs in the volume will consist of two independent velocities. In this limit, the relative velocity distribution and resulting intensity spectrum would be found by convolving the ordinary velocity distribution with itself.

To illustrate these results, let us suppose that $p(\vec{v}_1, \vec{v}_2|\vec{\Delta})$

has a bivariate Gaussian distribution. Although it is found experimentally that the distribution of turbulent velocities $p(\vec{v})$ is often Gaussian, it is generally recognized that higher order distributions are usually not Gaussian (see for example, Batchelor, 1953, p. 169). If a more refined analysis is needed, the Gaussian model we use here might be modified using Hermite polynomials as suggested by Frenkiel and Kelbanoff (1967).

To simplify things, let us suppose that v_1 and v_2 are the components of the vector velocities in the $\vec{K}$ direction, and assume that the mean velocity is zero.

We write for $p\ (v_1, v_2|\vec{\Delta})$

$$p\left(v_1, v_2 \,|\vec{\Delta}\right) = \frac{1}{2\pi\,\overline{v^2}\left[1-\alpha^2(\vec{\Delta})\right]^{1/2}} \times \exp - \frac{v_1^2 - 2\alpha(\vec{\Delta})v_1v_2 + v_2^2}{2\,\overline{v^2}\left[1-\alpha^2(\vec{\Delta})\right]} \quad , \tag{48}$$

where

$$\overline{v_1^2} = \overline{v_2^2} \equiv \overline{v^2} \ ,$$

and

$$\alpha(\vec{\Delta}) = \frac{\overline{v_1 v_2}}{\overline{v^2}} \ .$$

The spectrum can be found from equation (46) by substituting for $p\ (v_1, v_2, \vec{\Delta})$ the product $p\ (v_1, v_2|\vec{\Delta})\ p\ (\vec{\Delta})$ with $p\ (v_1, v_2|\vec{\Delta})$ given by equation (48). The result for the correlation $R_I(\tau)$ is

$$R_I(\tau) = \bar{I}^2\left[1 + \int d\vec{\Delta}\, p(\vec{\Delta}) \exp\left(-K^2\overline{v^2}\tau^2\left[1-\alpha(\vec{\Delta})\right]\right)\right] \quad ; \tag{49}$$

the spectrum is

$$S_I(f) = \bar{I}^2\,\delta(f) + \frac{\sqrt{\pi}}{K\sqrt{\overline{v^2}}}\int d\vec{\Delta}\, p(\vec{\Delta}) \frac{\exp\left[-\frac{\pi^2 f^2}{K^2\overline{v^2}\left[1-\alpha(\vec{\Delta})\right]}\right]}{\left[1-\alpha(\vec{\Delta})\right]^{1/2}} \quad . \tag{50}$$

These equations demonstrate the expected behavior when the velocity correlation length is made large or small with respect to the dimensions of the volume (to see this let α approach 0 or 1). In particular, when $\alpha = 0$, the spectrum is Gaussian with a HWHM of $\sqrt{\ln 2}\, K\sqrt{\overline{v^2}}/\pi$.

Nonhomogeneous situations and situations with non-zero mean velocities can be treated by using appropriate generalizations of the bivariate Gaussian distribution in place of equation (48). As an example, the general expression for the correlation $R_I(\tau)$ is

$$R_I(\tau) = \bar{I}^2 \left\{ 1 + \frac{1}{V^2} \int_V \int_V d\vec{r}_{11}\, d\vec{r}_{21}\, \exp\left[iK\tau \left(\bar{v}_1 - \bar{v}_2 \right) - K^2\tau^2 \left[\frac{\overline{v_1^2} + \overline{v_2^2}}{2} - \sqrt{\overline{v_1^2}\,\overline{v_2^2}}\, \alpha(\vec{r}_{11}, \vec{r}_{21}) \right] \right] \right\} \quad (51)$$

We have used this expression as the basis of a numerical calculation to obtain spectral widths to be compared with experimentally measured widths. The details of the calculation are taken up in section 14.

Finally, it should be noted that it is not difficult to construct a Gaussian model for the general situation in which the Lagrangian scale may be comparable to the length $1 / |\vec{K}|$. One simply writes a bivariate Gaussian distribution for $p(\rho_1, \rho_2 | \vec{\Delta})$ similar to equation (48) in which ρ_1 and ρ_2 are the components of $\vec{\rho}_1$ and $\vec{\rho}_2$ along $\vec{K}$. Upon substituting into equation (37A), one finds

$$R_I(\tau) = \bar{I}^2 \left\{ 1 + \int d\vec{\Delta}\, p(\vec{\Delta}) \exp\left[-K^2 \overline{\rho^2}(\tau) \left[1 - \alpha(\vec{\Delta}) \right] \right] \right\} \quad . \quad (52)$$

This expression reduces to equation (49) when $\overline{\rho^2} = \overline{v^2}\tau^2$.

III. EXPERIMENTAL STUDY OF A TURBULENT WATER JET

10. Introduction

The underlying idea in the experiment was to set up an optical homodyne in which light was scattered by some kind of uniform particle, verify that the homodyne was operating properly by observing the spectrum of the Brownian motion, and then study the effect on the spectrum of producing turbulence in the medium. To produce the turbulence, it was decided to use an underwater jet, water-into-water, a type of flow which is easily constructed and which has been extensively studied.* As with any type of non-homogeneous, shear-flow turbulence, mathematical analysis is somewhat difficult, but using an extrapolation of data published by Rosler and Bankoff (1963) concerning turbulent intensities and correlation lengths, and using the simple Gaussian model described in section 9, we compared calculated and measured widths. There seemed to be less turbulence than expected, but otherwise the measurements gave reasonable results. We have investigated the width of the homodyne spectrum as a function of jet velocity up to a Reynolds number of 7580, and have also investigated the spatial variation of the observed width at low Reynolds numbers for which the jet is partially laminar and partially turbulent. These observations will be described in this chapter.

---

*See, for example, Hinze, 1959, pp. 404-434, or Abramovich, 1963.

11. Description of the apparatus

The apparatus consisted of the jet and associated hydraulics, the laser, the photomultiplier, and the wave analyzers and other electronic equipment. The hydraulic system is shown in Fig. 2.

The jet nozzle was made by drilling out a .632 cm o.d. brass rod to an i.d. of .472 cm, and then drilling a .102 cm hole through the blank end as shown in the figure. The nozzle was inserted into a hole through a number 11 rubber stopper, and the stopper was used to plug one end of a 26 cm long glass-walled circular tube with an i.d. of 4.88 cm. Since the duct radius is approximately 24 nozzle diameters (ND), and since the jet radius (to the point where the axial velocity falls to half its maximum value) is less than 8 ND at the farthest point used for taking data (80 ND downstream from the nozzle), we have assumed that the jet behaves approximately as a free jet for the purpose of making calculations.

Water was circulated through the system using a small centrifugal pump, and the flow velocity was controlled with a needle valve and measured with a Gilmont size 13 calibrated flowmeter. The maximum nozzle Reynolds number* which we could obtain using the system was only 7580, but this was also about the upper limit for obtaining usable homodyne spectra. The system also included a reservoir with a thermometer for measuring the water temperature and a Fulflo 20 μ filter for removing unwanted particulate matter.

---

* $\frac{V_o d}{\nu}$, where d is the nozzle diameter, ν is the kinematic viscosity, and V_o is the exit velocity which we have taken to be $4Q/\pi d^2$, where q is the volume flowrate.

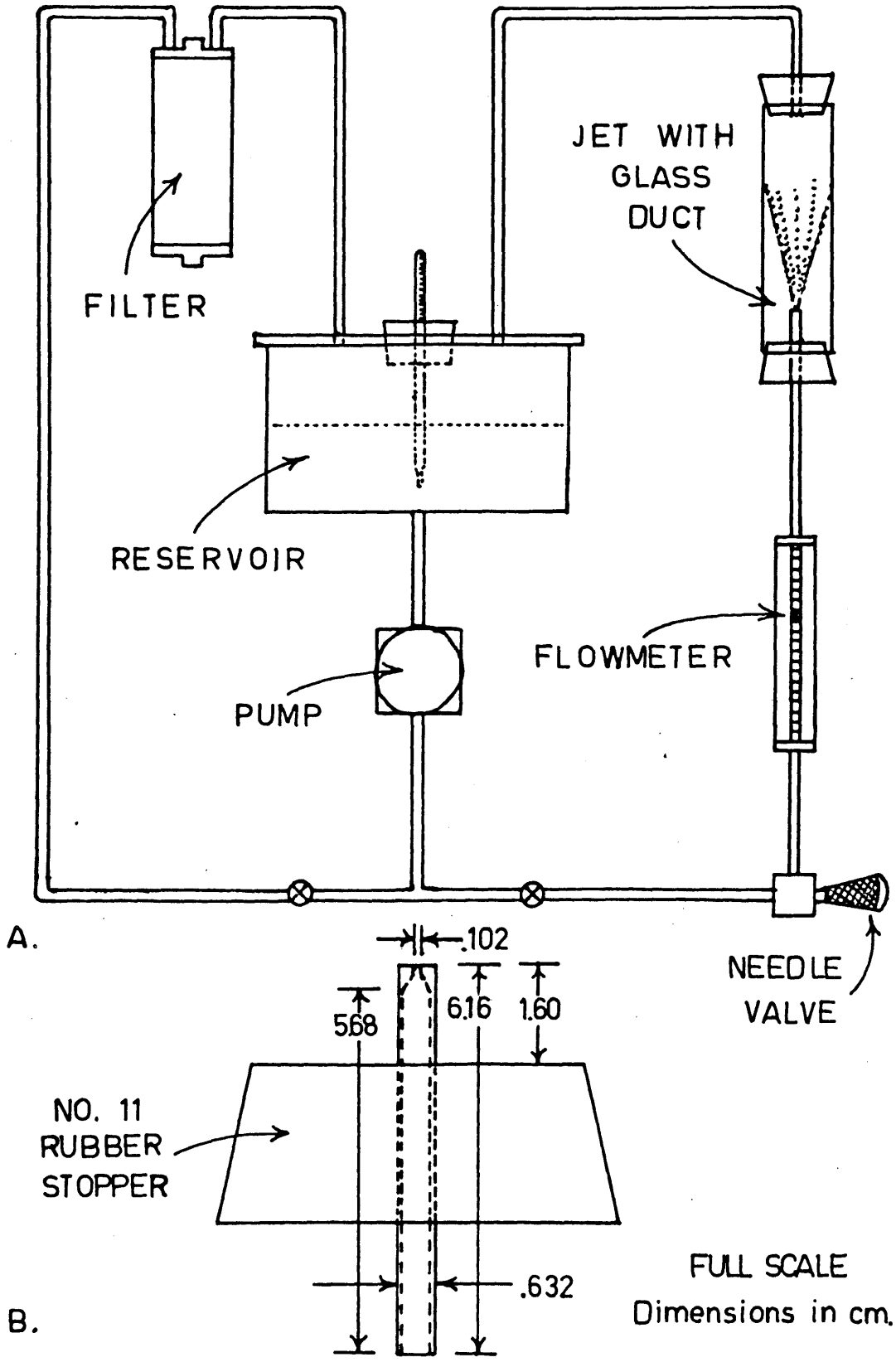

Fig. 2. Diagram of the hydraulics.

In order to observe the jet structure at the Reynolds numbers used in the experiment, Fluorescein dye was injected into the stream below the nozzle and photographs were taken of the marked fluid.

The transitional behavior of a jet in region of small Reynolds number is rather complicated, and has been studied by A. J. Reynolds (1962). The fully laminar jet breaks down in a "shearing puff" instability near the nozzle when $10 < Re < 30$, but as the Reynolds number is increased, a laminar-like length of jet returns and the unstable region moves progressively farther downstream. At Re = 380 for our jet (see Fig. 3) this thin, slowly spreading stream extended the full length of the duct. At still larger Reynolds numbers, the length of the laminar-like jet is reduced, the thin stream ending in an abrupt breakdown after which the jet spreads rapidly (see Fig. 4, Re = 630). As the Reynolds number is further increased, the length of the thin stream in reduced (Fig. 5, Re = 2530) until the jet becomes fully turbulent, spreading immediately after exiting from the nozzle (Fig. 6, Re = 5055). *

The Reynolds numbers used in our experiment ranged from 545 to 7580.

The scattering particles chosen to mark the jet were uniform spheres of polystyrene latex (available from the Dow Chemical Company) with a diameter of 910Å ± 6Å. The concentration of particles was roughly one part per thousand by volume. Since the particles tended to adhere to the walls of the reservoir and the hose, the system had to be cleaned from time to time. Fresh particles were always used when taking data.

The glass duct containing the jet was mounted on a three-dimensional positioning table so that the scattering volume could be located as desired. A picture of the apparatus showing the duct, laser

*The asymmetry of the jet apparent in these photographs is probably due to the bend in the hose leading to the nozzle.

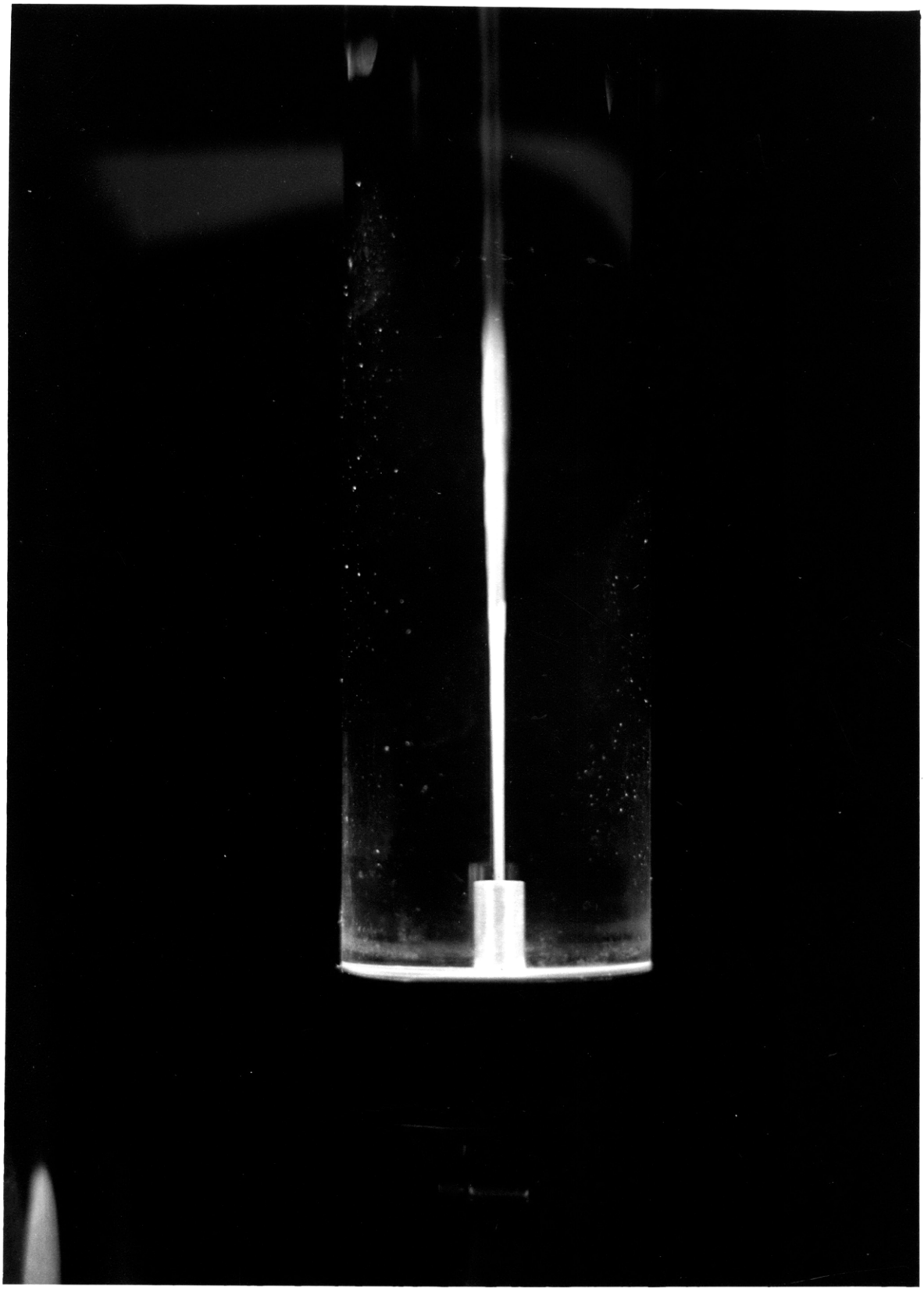

Fig. 3. Photograph of the jet. The Reynolds number is 380.

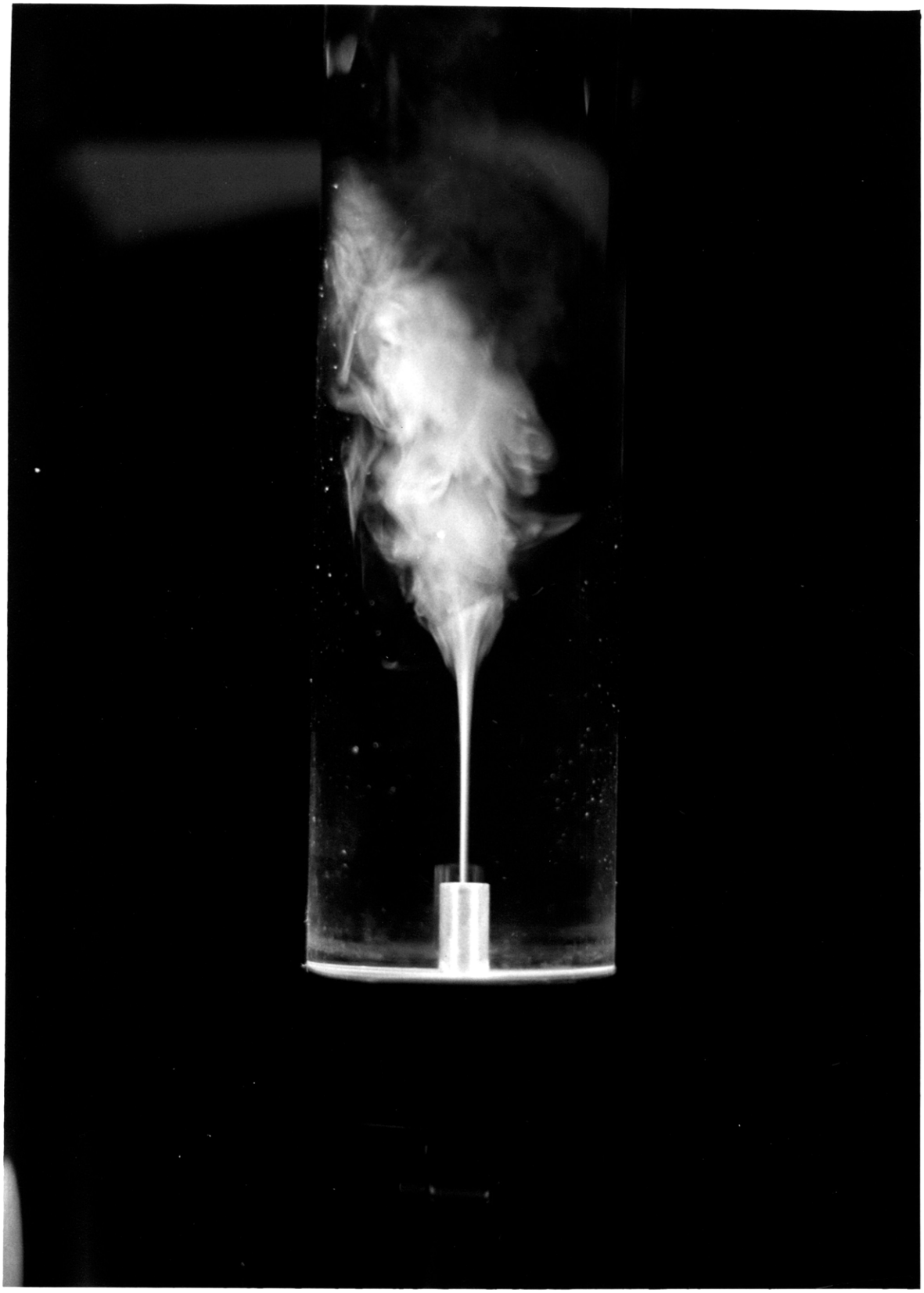

Fig. 4. Photograph of the jet. The Reynolds number is 630.

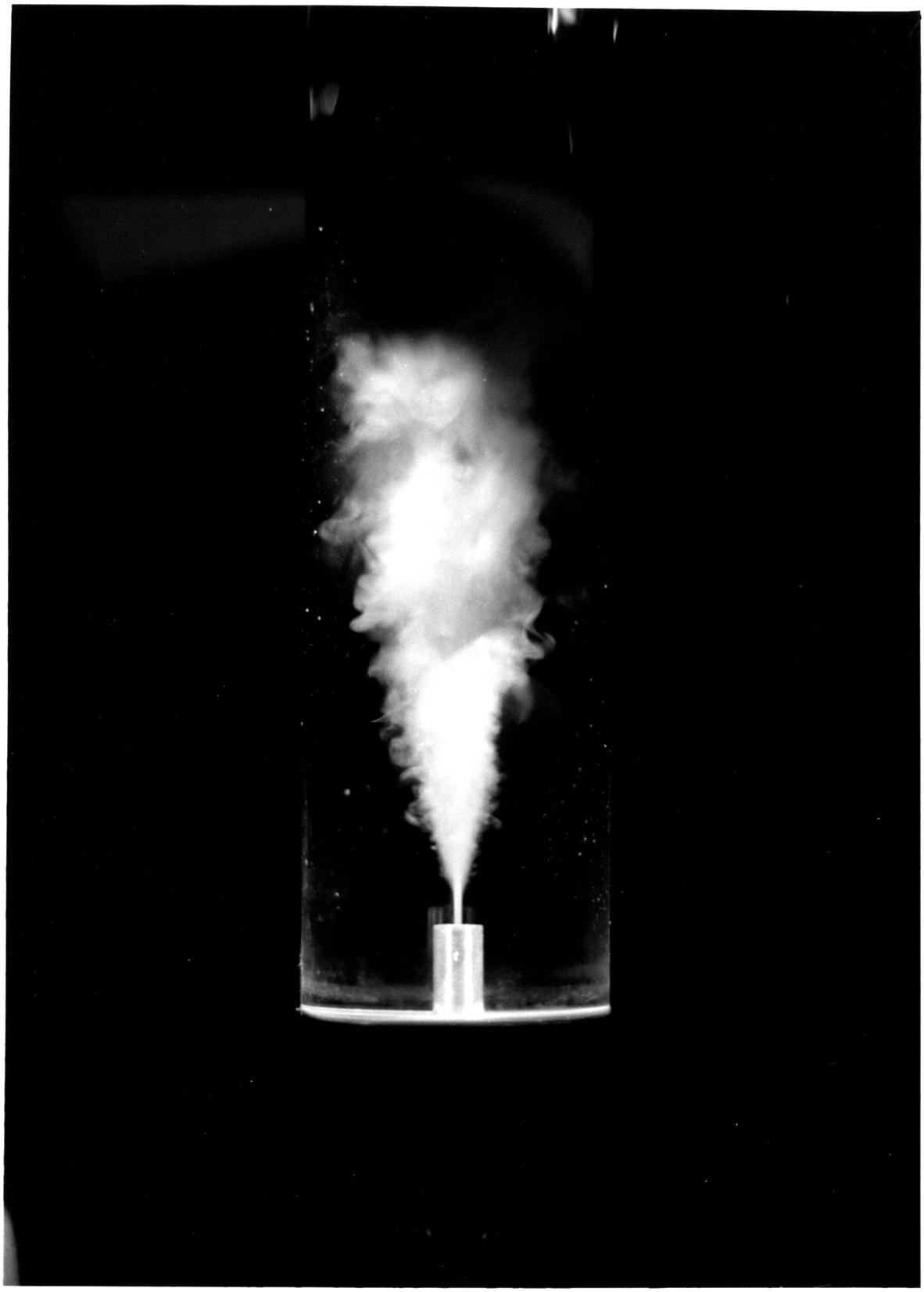

Fig. 5. Photograph of the jet. The Reynolds number is 2530.

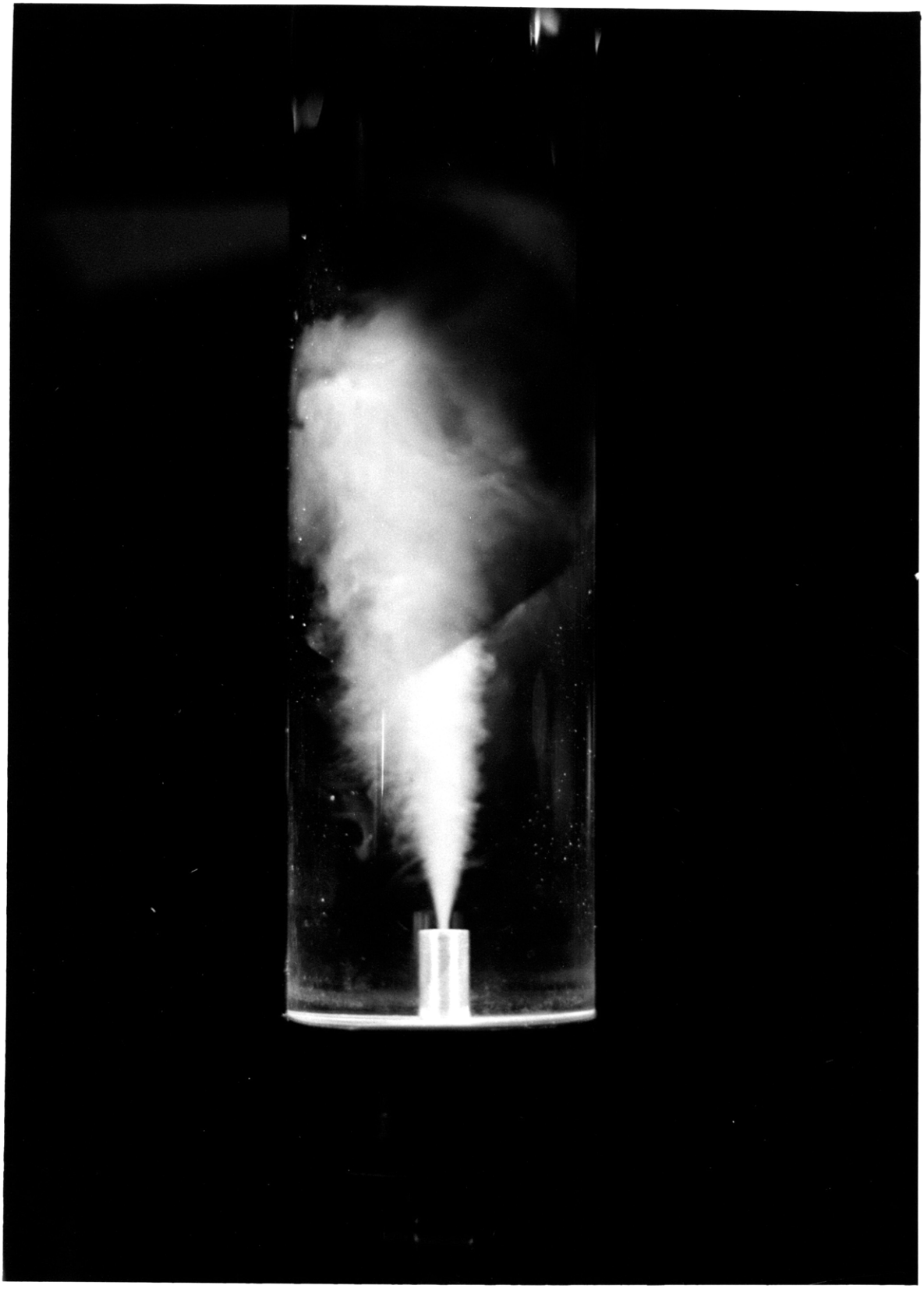

Fig. 6. Photograph of the jet. Reynolds number is 5055.

beam, and photomultiplier tube is shown in Fig. 7.

A diagram of the homodyne spectrometer is shown in Fig. 8.* The laser was a He-Ne Spectra Physics Model 120 with an output of 5.0 mw at a wavelength of 6328Å. The scattering was observed at an angle of 90° with an EMI 9558B photomultiplier placed one focal length away from a lens. An aperture was placed in front of the lens to limit the scattering volume, and a pinhole was placed directly in front of the cathode to control the range of scattering angle admitted, and to reduce the overall photocurrent to a convenient level. The size of the scattering volume was determined by shining the laser beam onto a fine wire placed in the scattering region and then observing the photocurrent while the wire was moved using the three-dimensional table. The scattering volume used in the experiment had a diameter of 4.0 ND.

One of the factors influencing choice of scattering volume size was a desire to avoid broadening the spectrum spuriously because of movement of the particles through the volume. ~~as discussed in sections 7 and 8 above~~. The largest velocity encountered in the experiment (at 80 ND with Re = 7584) was about .43 m/s. The transit time T in this case is 9.3×10^{-3}s and the spurious broadening which results for the homodyne is of the order (2/T) or 215 H_z. Since the measured width for this curve was 39.7 KH_z, the spurious broadening was neglected.

The anode resistor must be large enough so that the voltages generated across it are easily measured, but not so large that the

---

*A brief discussion of the signal-to-noise ratio for the homodyne spectrometer will be found in Appendix V.

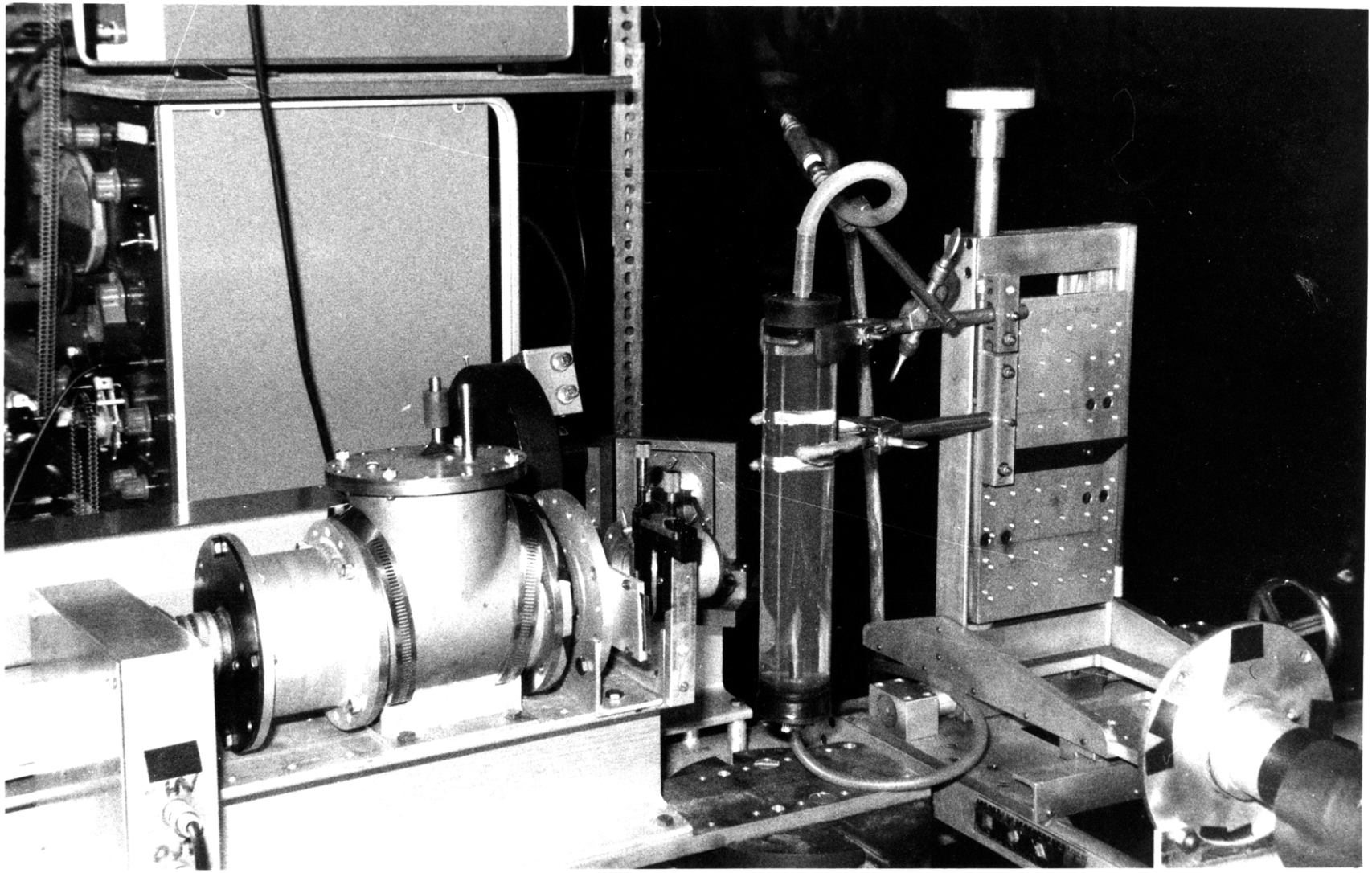

Fig. 7. Photograph of the apparatus.

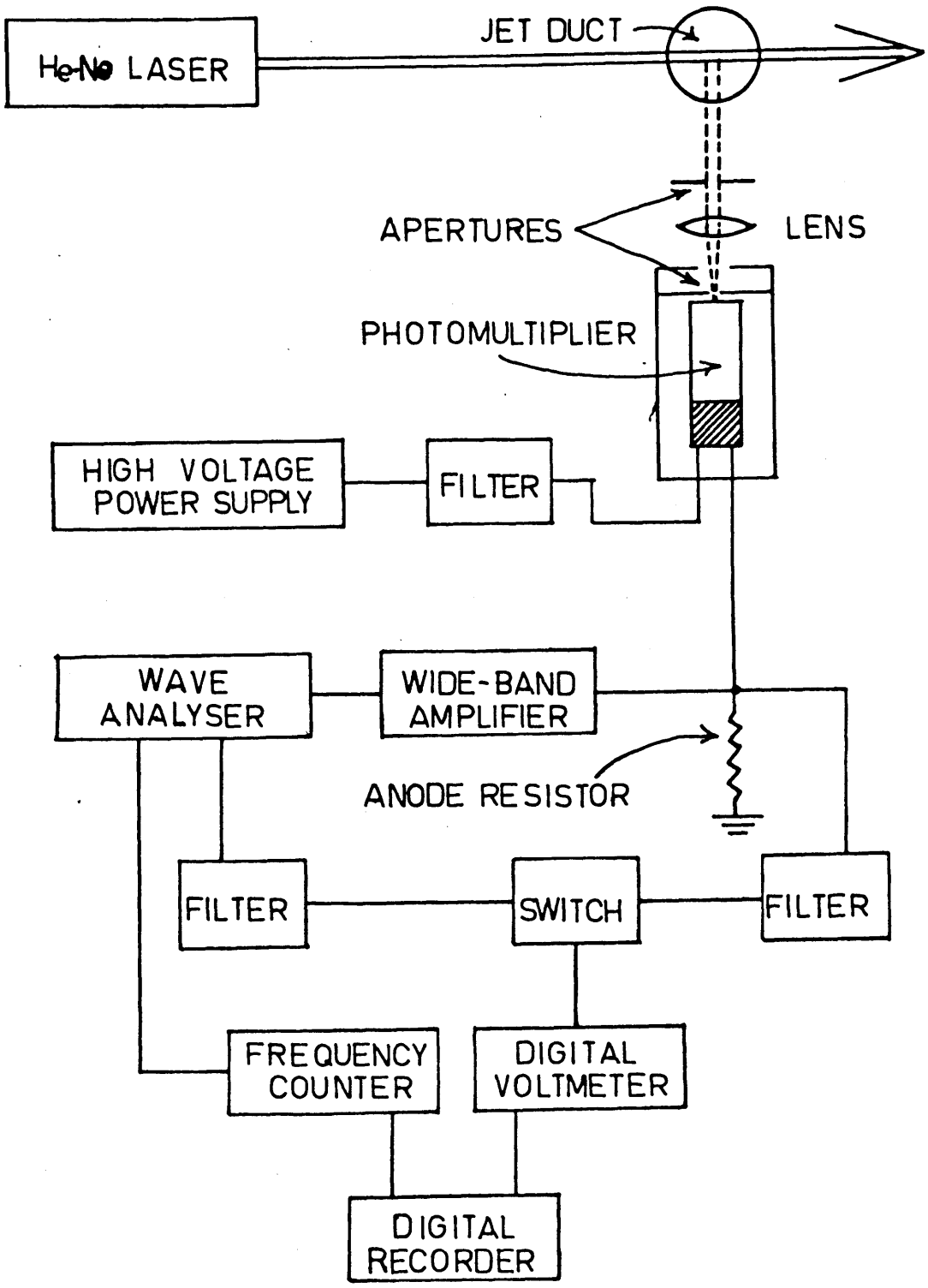

Fig. 8. Diagram of the spectrometer.

frequency response of the photomultiplier over the range of frequencies being measured is affected. A value of 619 Ω was used in our experiment, and it was found that the shot-noise power at 430 Khz was 90% of its low frequency value. The response was sufficiently flat in the 0 - 50 Khz region.

Three quantities were recorded at intervals.

The mean value of the photocurrent was monitored by measuring the voltage across the anode resistor with a Hewlett-Packard 3440A digital voltmeter (3443A high-gain plug in) coupled with a low-pass filter. The photocurrent amplitude spectrum (square root of the power spectrum) was measured using one of two wave analyzers, a General Radio 1900A for spectra having widths less than about 10 Khz, and a Hewlett-Packard 310A for wider spectra up to about 40 Khz. A Tektronix type CA preamplifier in a type 132 unit power supply was used to amplify the voltage generated across the anode resistor before detection with the wave analyzer, and the wave analyzer output after detection was fed to the digital voltmeter through additional external filtering and a mechanical switching device. The digital voltmeter alternated between a reading of the mean photocurrent and a reading of the voltage spectrum. The frequency of the wave analyzer was monitored using an electronic counter (Hewlett-Packard 5216A) connected to the BFO terminal. The readings of the digital voltmeter and the counter were printed at one second intervals using a Hewlett-Packard 562A digital recorder.

12. Analysis of the printed data

The printed data together with measured shot-noise levels were punched onto IBM cards for analysis with a digital computer. The computer was programmed to carry out some arithmetical operations, and then to make a least squares fit of the measured spectrum to a rational function. Output information included the parameters of the least squares fit, and the frequency at which the fitted curve had fallen to half of its zero frequency value.

The arithmetical operations were as follows. The wave analyzer voltage output was squared to obtain a quantity proportional to the spectral power; the result was divided by the mean photocurrent to compensate for a gradual decrease (and other small changes) observed in the photocurrent;* the shot-noise power as measured at a high frequency and compensated for roll-off was then subtracted; finally, the result was again divided by the mean photocurrent. The rationale behind dividing a second time by the mean photocurrent may be seen from equation (1): the shot-noise power is proportional to the mean photocurrent, but the homodyne spectrum is proportional to the square of the mean photocurrent.

The least squares fit was made to a rational function of the form $1/(a_o + a_1 f^2 + a_2 f^4)$, where f is the frequency, and a_o, a_1, and a_2 were parameters to be determined. The size of the parameter a_2 was an

*This decrease was ascribed to a decrease in the particle concentration due to gradual adhesion to the walls of the apparatus. The laser power was not monitored, but it is unlikely that it fluctuated very much.

indication of whether or not the experimental points lie on a Lorentzian curve. The actual procedure was to fit the reciprocals of the data points to the quadratic (in f^2) function ($a_o + a_1 f^2 + a_2 f^4$) using the analytic solution to the normal equations. The reciprocal data points were weighed so that the actual data points would contribute equally in determining the fit.

13. Observed spectrum when particles undergo Brownian motion

The apparatus was tested by observing the width and shape of the spectrum when the jet was turned off and the particles underwent Brownian motion. According to the theory given in section 8 above, the curve should have a Lorentzian shape centered at zero frequency with a half width at half maximum (HWHM) of K^2D/π hz. The diffusion coefficient D can be calculated from the Stokes-Einstein relation, equation (41).

The data points obtained in this case at 28°C with a 50 hz bandwidth are shown in Fig. 9. This spectrum took about 90 minutes to record. The least-squares fitted curve had a width of 674 hz. A Lorentzian having this width is shown in the figure and it may be seen that the agreement is quite good.

The diffusion coefficient (adjusted to 25°C) obtained from this data was $(5.74 \pm .15) \times 10^{-12}$ m^2/s. The value calculated from equation (41) was $(5.34 \pm .30) \times 10^{-12}$ m^2/s, the variance in the figure being due to the variance in the particle sizes. Dubin, Lunacek, and Benedek (1967) measured a value of $(5.9 \pm .2) \times 10^{-12}$ m^2/s at 25°C for slightly smaller particles (d = 880A). It was concluded that the agreement between theory and experiment was satisfactory, and that the homodyne spectrometer was working properly.

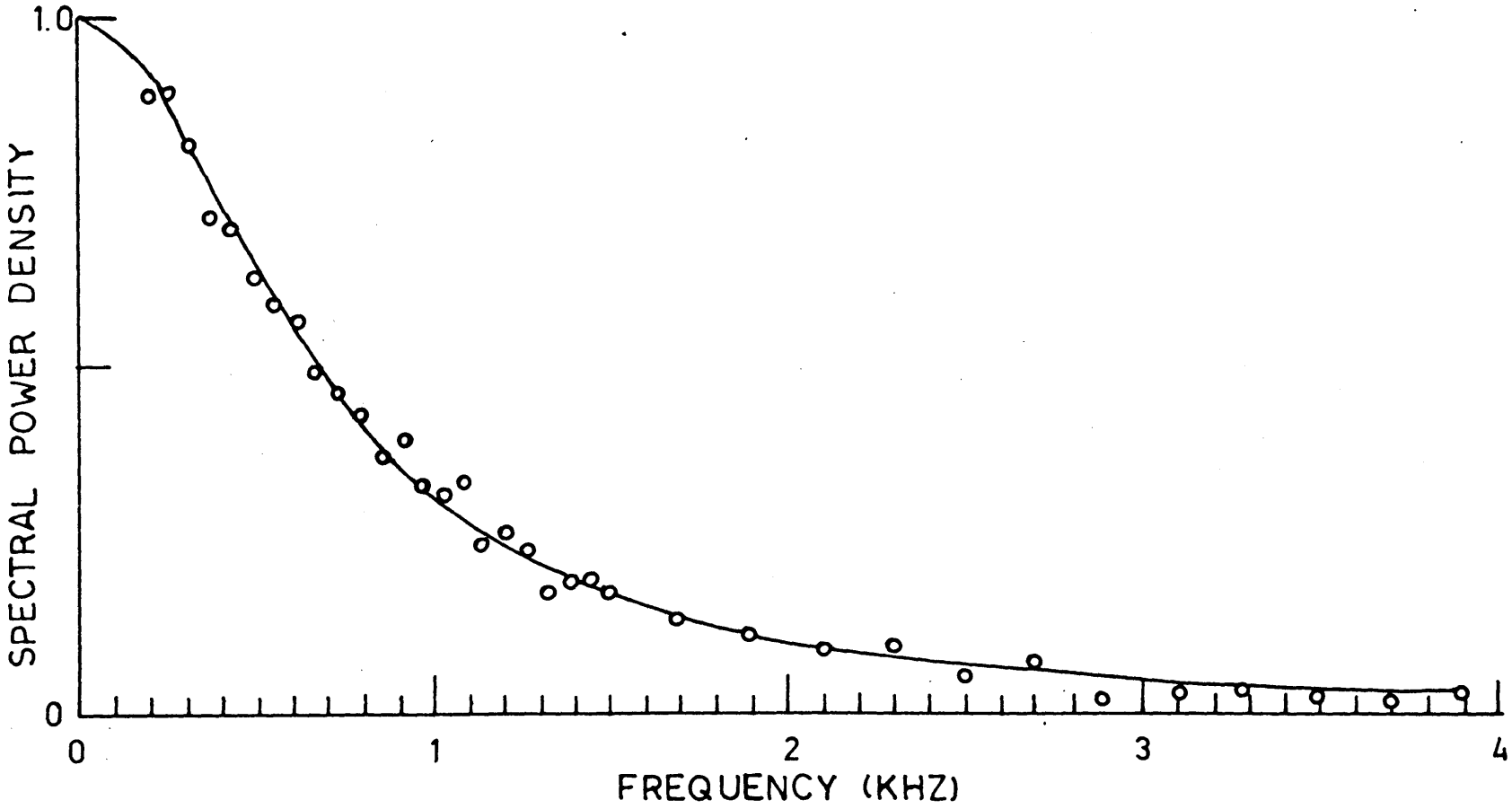

Fig. 9. Spectrum of light scattered from spheres of 910 Å diameter undergoing Brownian motion in a water solution. Solid curve is Lorentzian with 674 Hz width.

14. Observed spectrum as a function of velocity and position in the jet

When the jet was turned on, the spectrum was observed to broaden. In order to guard against the possibility that the broadening was being caused by gross concentration fluctuations due to the turbulence, the observation was repeated using an incoherent light source. In this case only the flat shot-noise spectrum was observed. It was concluded that the spectrum being observed with the laser source was indeed a homodyne spectrum.*

The broadening observed using the laser source was quite large and it was necessary to keep the fluctuation velocities small in order to obtain spectra with measurable widths. For this reason, the behavior of the spectrum as a function of velocity was investigated reasonably far downstream (80 ND). The behavior of the spectrum as a function of position was investigated at a maximum Reynolds number of 660. The results obtained were quite reasonable, but a detailed comparison with theory was difficult because of uncertainties about the turbulent intensities at low Reynolds numbers and as far downstream as 80 ND.

The behavior of the jet as a function of velocity is shown in Figs. 10, 11, and 12. The scattering volume was located on the axis of the

---

*The author's experience suggests that this check should always be carried out when mixing experiments are done with turbulent fluids. A very similar light scattering technique which measures spectra of concentration fluctuations has been described by Becker, Hottel, and Williams (1967). Such spectra have been observed by the present author in scattering experiments on jets of steam. The spectra are similar in appearance to homodyne spectra, but are observed with both incoherent and coherent light. Homodyne spectra are, on the other hand, not observed with incoherent light sources under ordinary circumstances.

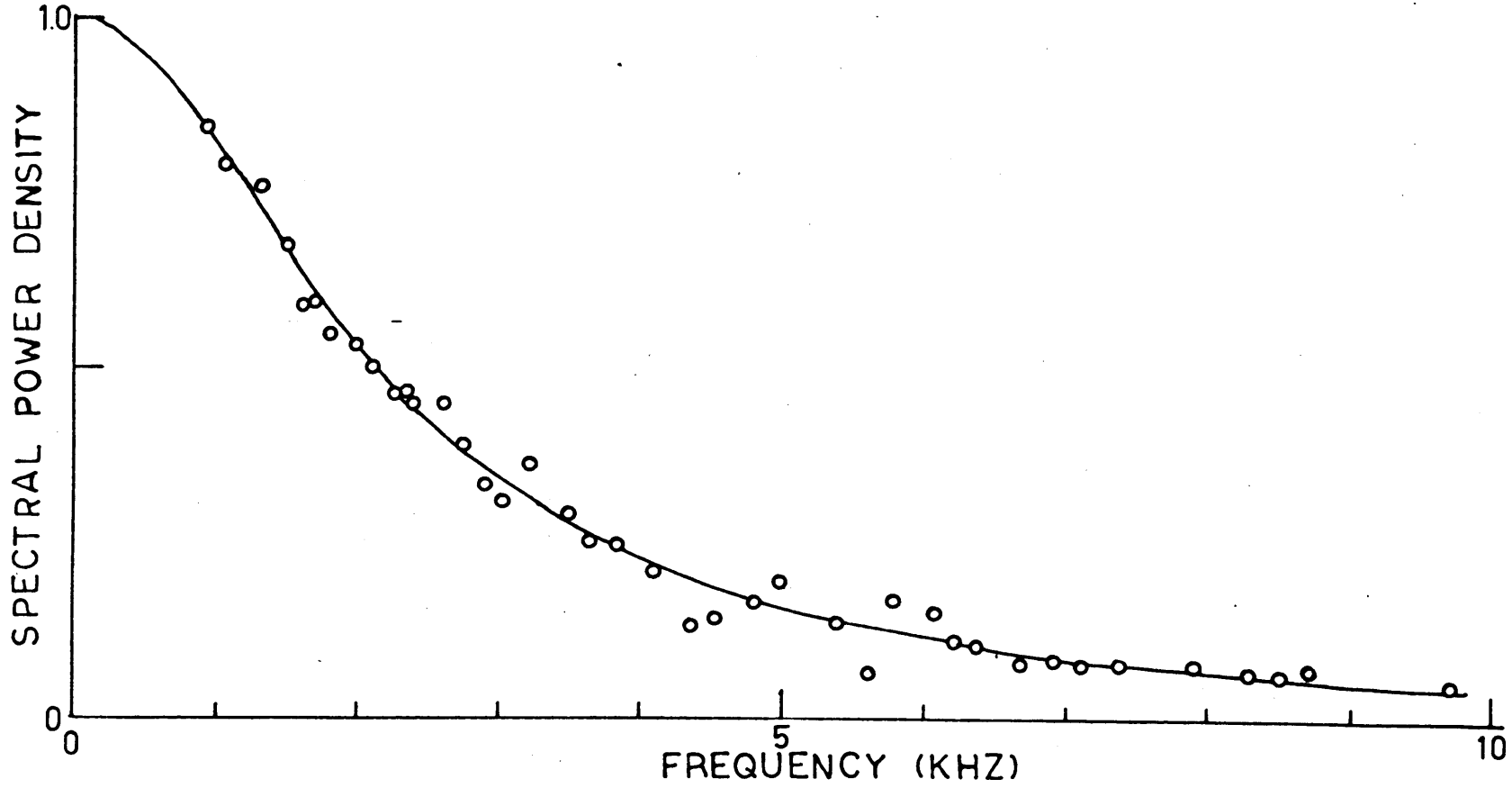

Fig. 10. Spectrum of light scattered from 910 Å diameter spheres suspended in a turbulent water jet. Scattering volume is on the axis, 80 nozzle diameters downstream from the nozzle. Reynolds number: 505. Solid curve is Lorentzian with 2.16 Khz width.

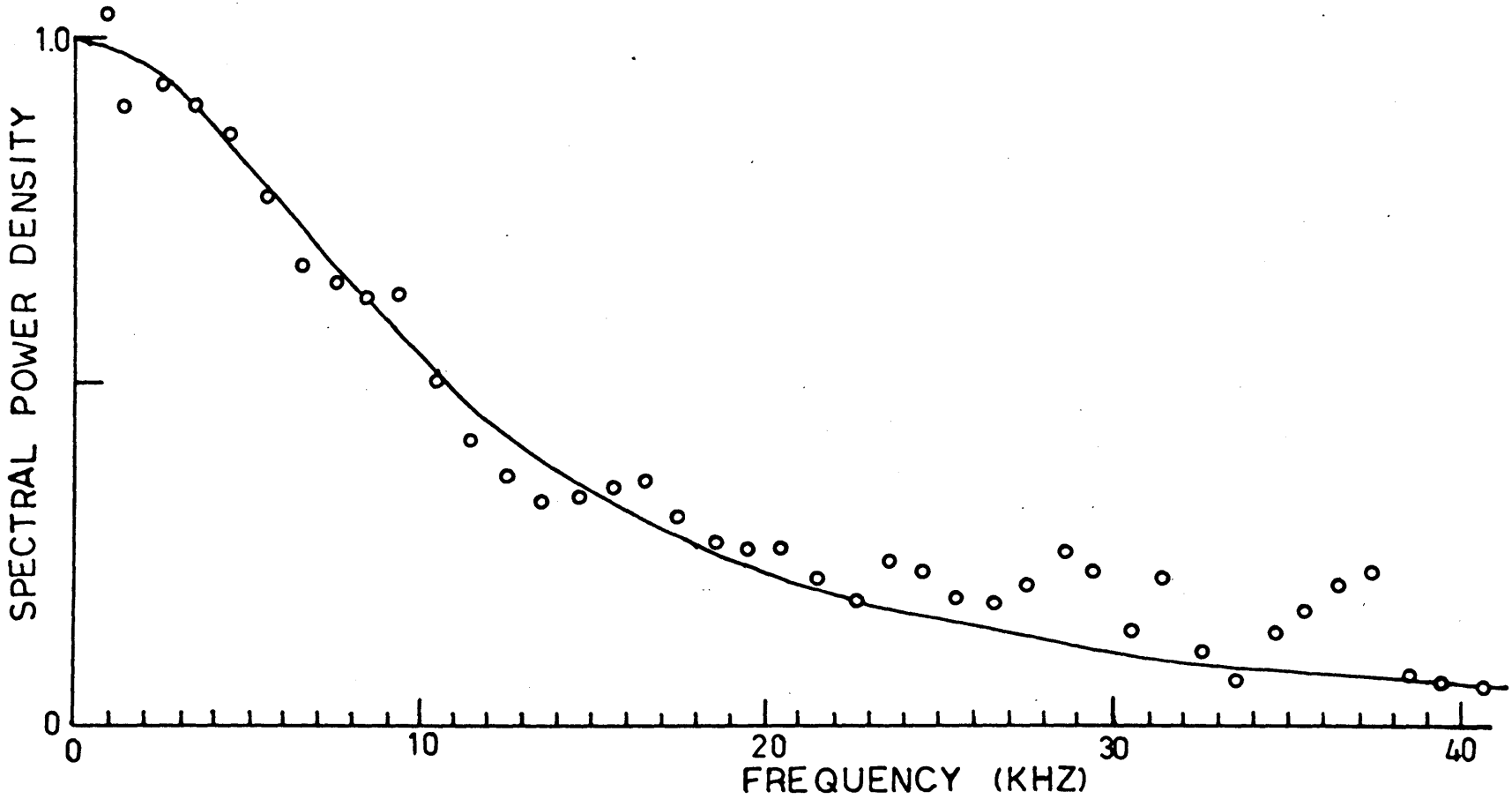

Fig. 11. Spectrum of light scattered from 910 Å diameter spheres suspended in a turbulent water jet. Scattering volume is on the axis, 80 nozzle diameters downstream from the nozzle. Reynolds number: 2530. Solid curve is Lorentzian with 10.78 Khz width.

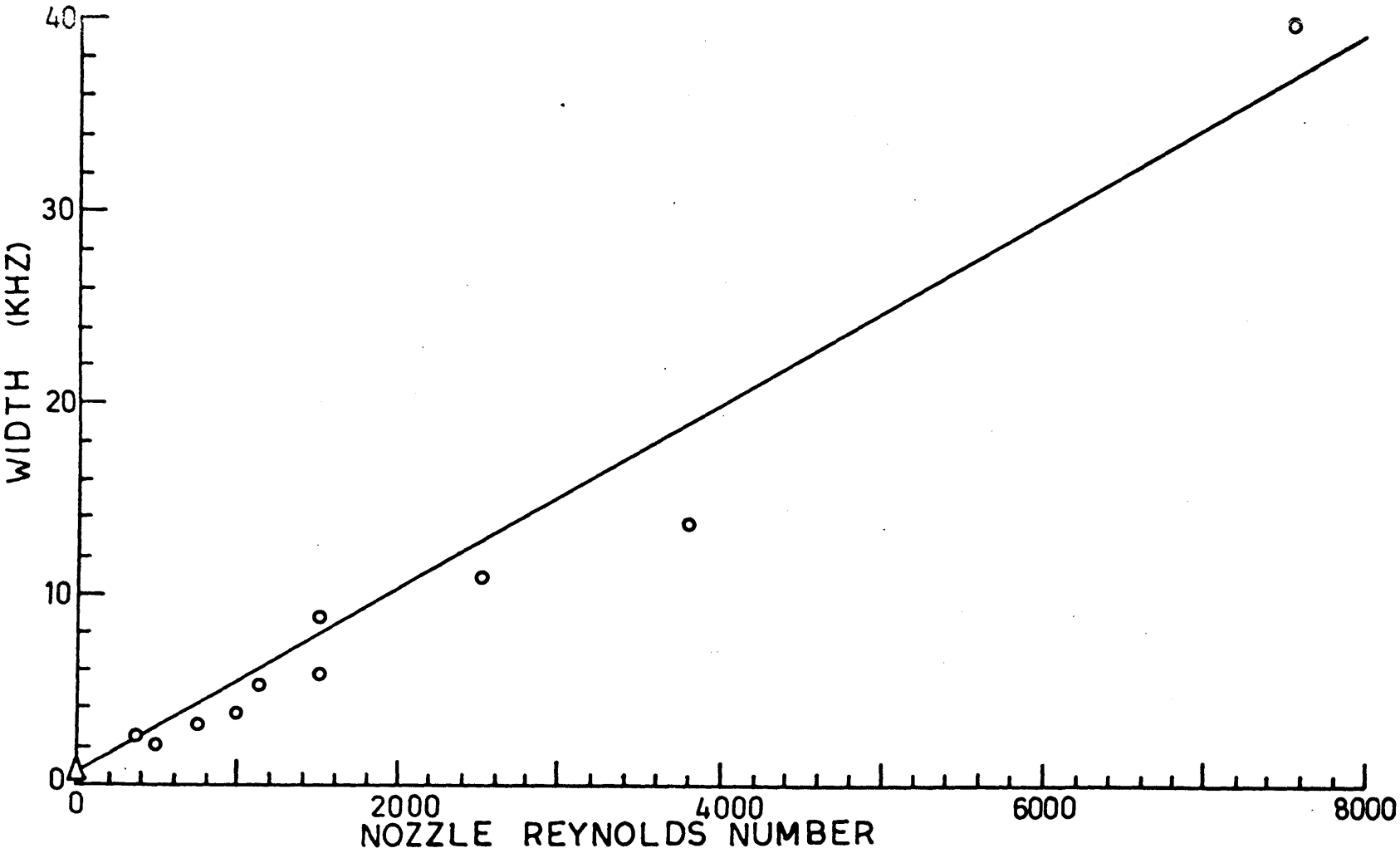

Fig. 12. Width of the scattered spectrum as a function of jet nozzle Reynolds number. Data were taken on the axis of the jet, 80 nozzle diameters downstream from the nozzle.

jet, 80 ND downstream. Fig. 10 shows a spectrum obtained with a bandwidth of 200 hz when Re = 505. The smooth curve is a Lorentzian having a width of 2.16 KH_z. Fig. 11 shows a spectrum obtained with a bandwidth of 200 hz when Re = 2530. The smooth curve in this case is a Lorentzian having a width of 10.78 Khz. In general, the measured curves tended to be more Lorentzian in shape than Gaussian.

The width of the spectra is shown plotted as a function of Reynolds number ~~flow rate~~ in Fig. 12 (300 ml/min corresponds to Re = 7585). The straight line represents a least-squares fit. The widest curve (Re = 7585) had a width of 39.7 KH_z and was measured with a 1 KH_z bandwidth.

In order to compare these results with the theory of section 9, a numerical integration of the correlation function equation, equation (51), was carried out using a digital computer. The geometry is such that only radial components of the velocity are detected. The turbulent fluctuation velocity gradients are usually much larger than the radial mean velocity gradients, so that the latter have been neglected. The two volume integrals were replaced by two one-dimensional integrals in the radial direction. The velocity correlation function $\alpha(\Delta)$ was chosen arbitrarily to be either exponential

$$\alpha(\Delta) = e^{-\frac{\Delta}{L}}, \tag{53}$$

or Gaussian

$$\alpha(\Delta) = e^{-\frac{\pi\Delta^2}{4L^2}}, \tag{54}$$

where L is the integral scale (Hinze (1959), p. 41). The input data (Eulerian) consisted of the turbulent intensities as a function of radial position, the nozzle velocity V_0, the integral scale L, the location and size of

the scattering interval, and the time τ at which $R_I(\tau)$ was to be evaluated initially. The computer calculated the value of the double integral, then chose a new value of τ and repeated the calculation until it found the first value of the time τ_0 for which the double integral had fallen to half of its maximum value plus or minus 1 percent. The HWHM of the spectrum in hz was taken to be $\ln 2/2\pi\tau_0$, as it would be if the correlation function were a simple exponential.

Information on turbulent intensities and integral scales in a water-into-water jet was taken from Rosler and Bankoff (1963). One of the interesting features of jet turbulence is the fact that the radial distribution of the axial component of the turbulent intensity becomes self-preserving (maintains a similar form determined only be a length scale and a velocity scale) beyond about 30 ND downstream from the nozzle. Radial profiles of the turbulent intensity in the self-preserving region are roughly Gaussian in shape with the intensity on the axis being given by

$$\frac{v'}{V_o} = 1.72 \frac{d}{z + z_o} , \tag{55}$$

where v' is the rms turbulent velocity, V_o is the nozzle velocity, d is the nozzle diameter, z is the distance from the nozzle, and z_o is the distance to the geometrical origin of the jet (usually less than a nozzle diameter in front of the nozzle; for Rosler and Bankoff, $z_o/d = -0.9$). The HWHM of the curve is given roughly by

$$(\Delta r)_{1/2} = .108 (z + z_o). \tag{56}$$

The radial component of the turbulent velocity fluctuation is known to be of approximately the same magnitude as the axial component (Hinze, 1959, p. 434). The radial component of the turbulent intensity at 80 ND required for our theoretical calculation was obtained therefore by

using the data supplied by Rosler and Bankoff for the axial component at 30 ND together with the scaling laws (55) and (56).

The laterial integral scale for jets as given by Rosler and Bankoff can be determined approximately from the relation (we have chosen the value for jets in which there is no free surface)

$$L = .076\ (z + z_o)\ , \tag{57}$$

At $z/d = 80$ and with $z_o/d = -0.9$, $L/d = 6.01$.

The width calculated using the exponential velocity correlation, equation (53), for a flow rate of 100 ml/min (Re = 2530) was 45.8 Khz. The Gaussian velocity correlation, equation (56), at the same flow rate gave a width of 19.7 Khz. The measured width was 13.0 Khz. The data would seem to indicate less turbulence present than expected on the basis of the extrapolation from the measurements of Rosler and Bankoff.

There are several possible explanations for this result.
1. The particles might be affecting the turbulence. A study by White (1967) on jets formed by polymer solutions showed that adding certain polymers to a water jet caused the jet to spread at a greater angle so that the center-line velocity was reduced. One might expect a similar reduction in the fluctuation velocities. 2. The effect of the duct might not be negligible as far downstream as 80 ND. The ducted jet grows faster than the free jet (Becker, 1961), so that the center-line velocity would also be reduced. 3. The turbulence may not be self-preserving as far downstream as 80 ND, so that the use of equations (55) and (56) may not be justified. It would seem that the best way to resolve these uncertainties would be to measure the turbulent fluctuation velocities directly.
4. The problem may be due to our having replaced the volume integrals in

equation (51) with one-dimensional integrals in making the calculation. This would tend to overemphasize the importance of volume elements lying on a line passing through the axis of the jet and might cause the calculated spectrum to be too wide.

The other experimental project undertaken was to investigate the behavior of the spectrum as a function of position. The Reynolds numbers used were in the range of 505 to 660 so that the jet was not fully turbulent but had a structure similar to that shown in Fig. 4 (Re = 630).

In order to allow a large number of positions to be investigated easily and quickly, the spectral power was measured in a 50 hz bandwidth centered at 300 hz as the position of the scattering volume was scanned radially and axially. For curves with a width of several kilohertz, the spectral power at 300 hz is effectively a measure of the height of the curve. If it is assumed that the spectrum has a Lorentzian shape and that the total power is constant, then the product of width and height will be constant. Thus, an effective width may be obtained by measuring the height.

Fig. 13 shows a full spectrum obtained when the scattering volume was on the axis of the jet at 40 ND with Re = 505. The solid curve is a Lorentzian with a width of 8.48 Khz. This curve was used to determine the product of width and height.

The spectrum in Fig. 13 was taken under identical conditions to the spectrum shown in Fig. 10 except that the scattering volume was at 40 ND instead of 80 ND. Thus, the turbulent fluctuation velocities appear to increase as one goes closer to the nozzle. That this trend does not continue as one moves closer to the nozzle than 40 ND is indicated in Fig. 14, where the width of the spectrum (determined from the height) is

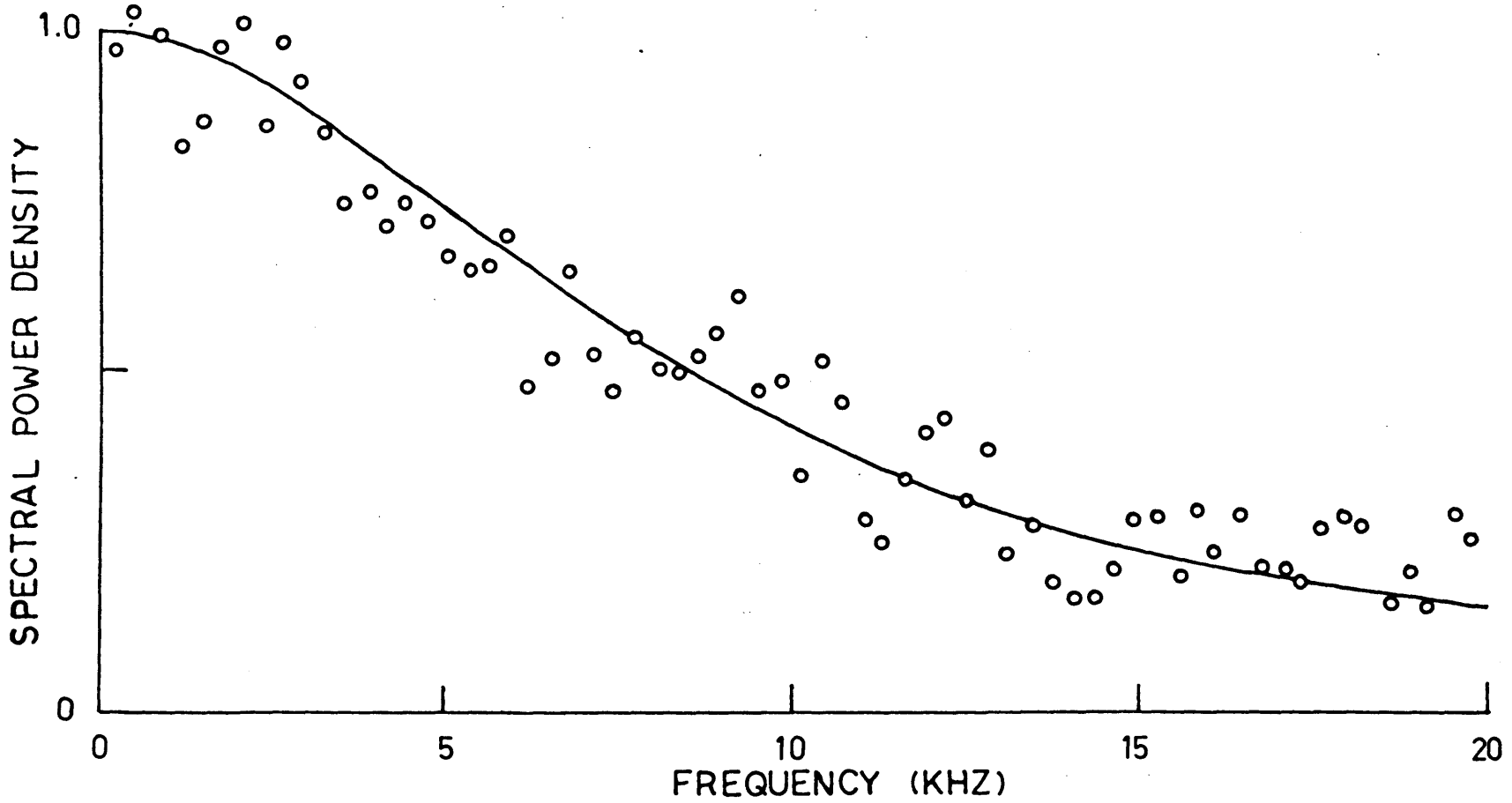

Fig. 13. Spectrum of light scattered from 910 Å diameter spheres suspended in a turbulent water jet. Scattering volume is on the axis, 40 nozzle diameters downstream from the nozzle. Reynolds number: 505. Solid curve is Lorentzian with 8.48 Khz width.

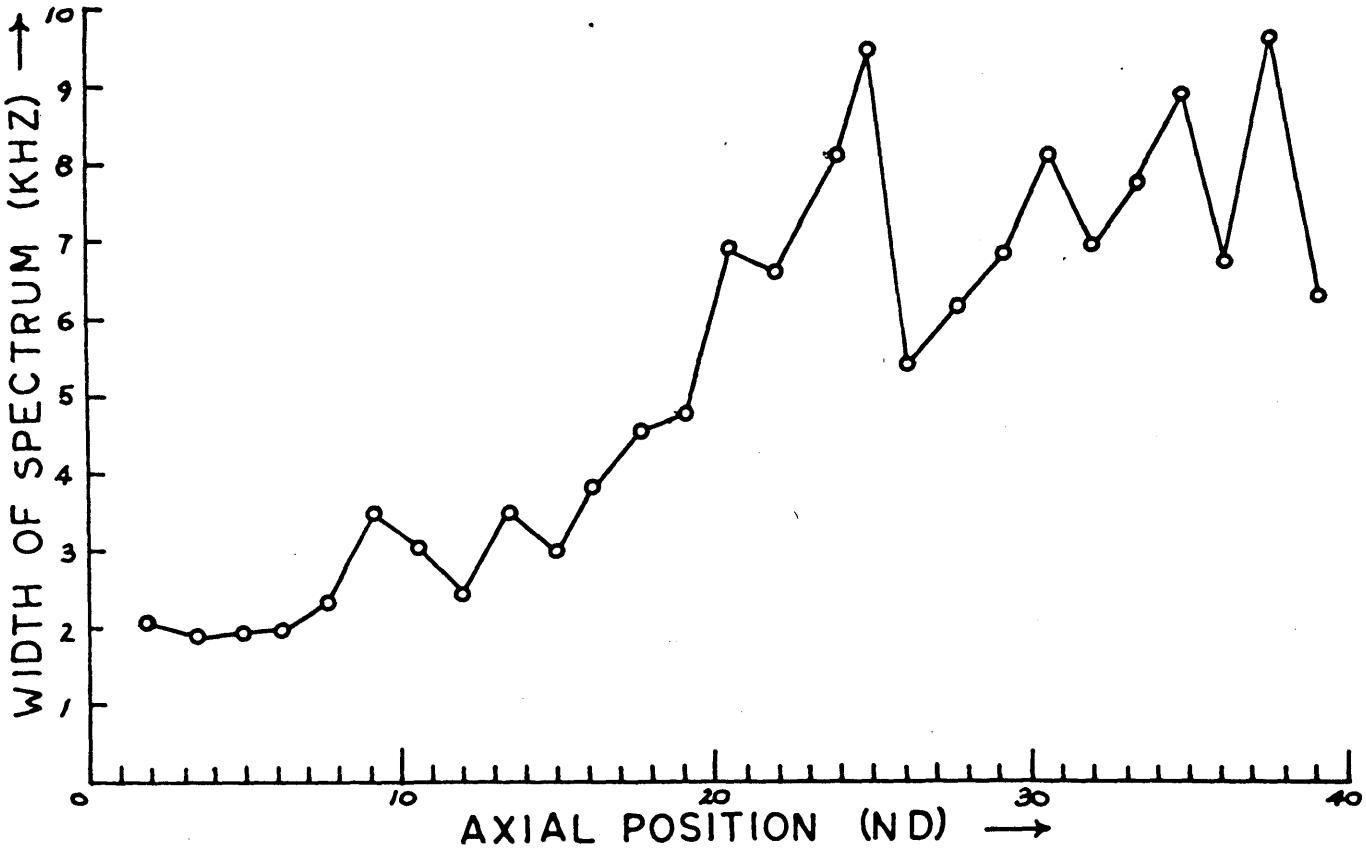

Fig. 14. Width of the scattered spectrum as a function of axial position in nozzle diameters. Reynolds number: 505.

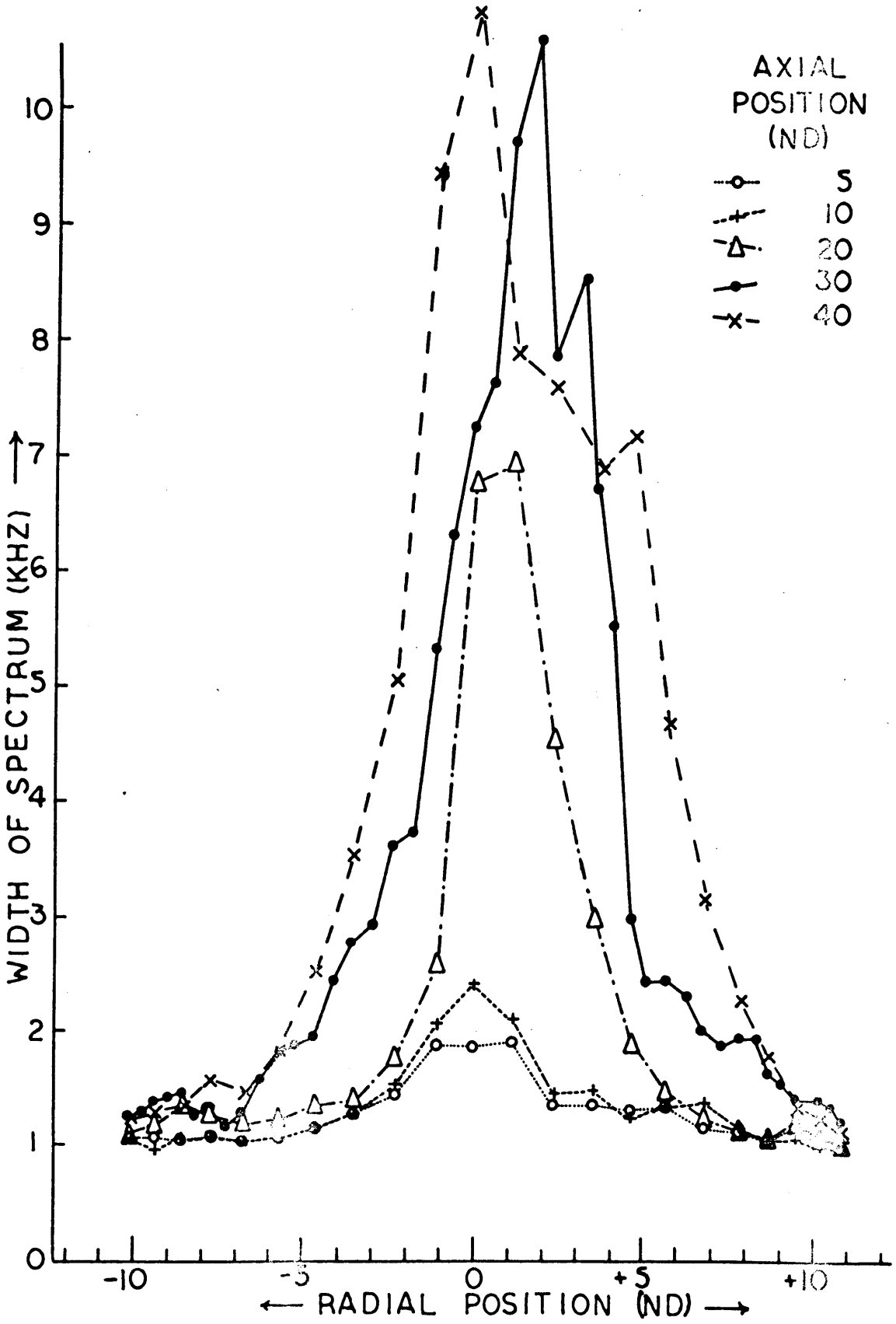

Fig. 15. Width of the scattered spectrum as a function of radial position at selected axial positions. Reynolds number: 660.

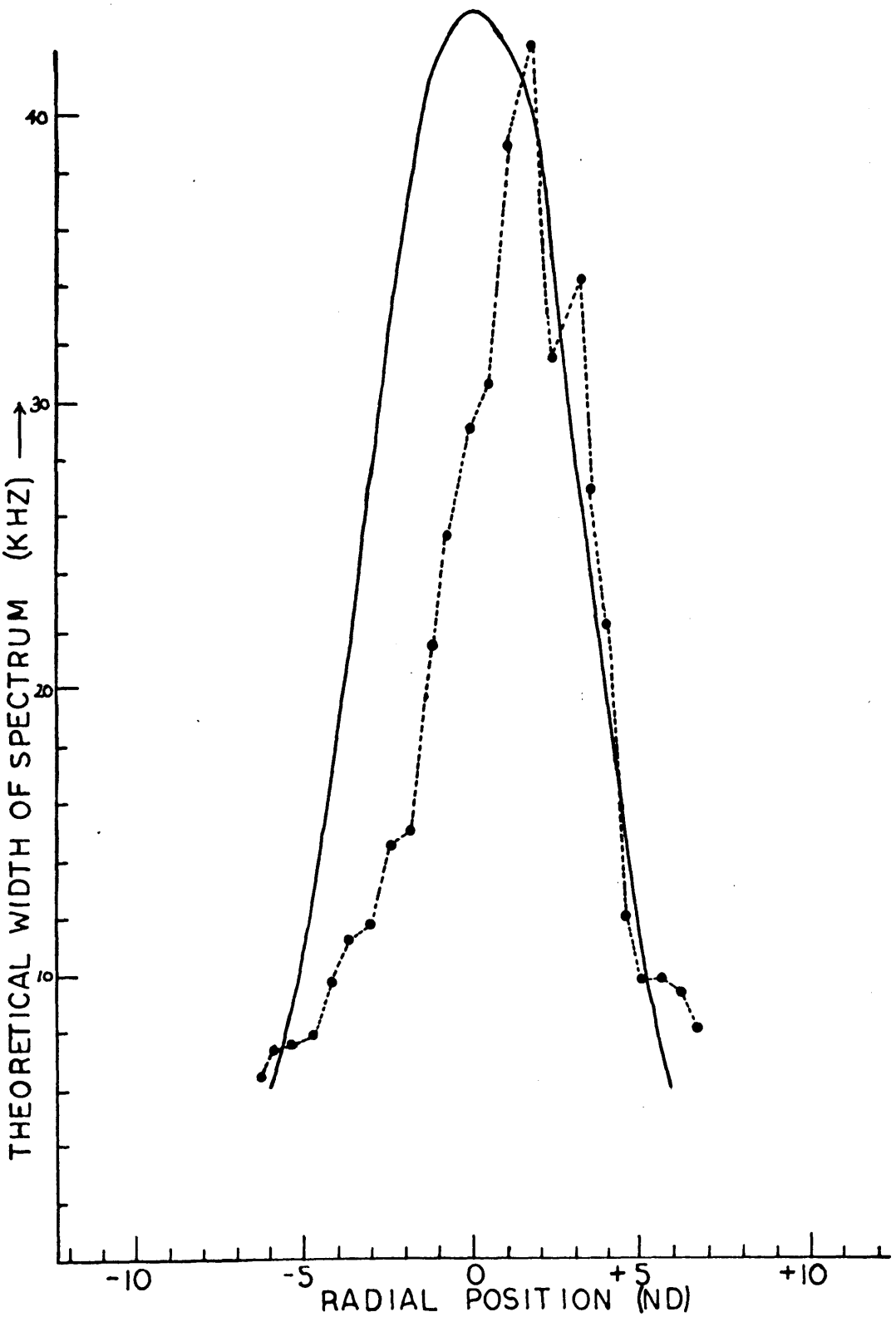

Fig. 16. Solid curve is the theoretical width of the spectrum from a fully turbulent jet. Dashed curve is the experimental width of the spectrum (times 4) from a partially turbulent jet. In both cases the axial position is 30 nozzle diameters from the nozzle.

plotted as a function of axial position. The apparent decrease in the turbulence is reasonable in view of the laminar-like flow which is observed to occur in this region (see Fig. 4).

A set of five radial scans at axial positions of 5, 10, 20, 30, and 40 ND respectively is shown in Fig. 15. The width of the spectrum is shown plotted as a function of radial position. The growth of the turbulence with increasing axial distance is apparent, as is the spread of the jet. Corrections have been applied to the data to take into account the refraction which occurs at the curved surface of the glass duct.

Fig. 16 shows a theoretical curve at 30 ND based on the Gaussian model calculation for a fully turbulent flow. The curve was obtained using an exponentially decaying velocity correlation law (equation (53)), and is shown merely to indicate the shape of the curve one might expect for the fully turbulent jet. The experimental points plotted on an expanded vertical scale are seen to describe a somewhat narrower, more pointed curve. The asymmetry of the experimental points corresponds to the asymmetry of the jet which is evident in the photographs, and is believed to be due to the bend in the hose leading to the nozzle.

IV. CONCLUSIONS

15. Summary of results

We have made a theoretical and experimental study of the homodyne spectrum of light scattered from particles suspended in a turbulent fluid. The principal theoretical result of this paper is equation (37B) for the spectral density of the scattered intensity; this equation is useful for situations in which particle motions are not independent. In most scattering experiments involving turbulence, the Lagrangian integral scale will be large compared with $1/|\vec{K}|$, where $\vec{K}$ is the vector difference between incident and scattered wavevectors, and equation (37B) can be written in terms of the two-particle, relative velocity distribution as in equation (47). Experimentally, we have been able to observe spectral broadening due to velocity fluctuations in a turbulent jet. It was possible to observe the transition from a diffusion-broadened spectrum to a turbulence-broadened spectrum by varying the position of the scattering volume within the jet and by varying the jet nozzle velocity. A numerical calculation based on both the above theory and measurements on similar jets by other investigators indicated that less turbulence was present than expected for a free jet of pure water; simultaneous measurements by other means of the turbulence parameters are needed to resolve this problem. Nevertheless, the experiment was useful to demonstrate the possibility of the measurement and indicate the type of results which can be obtained.

16. Suggestions for future experiments

There are a number of suggestions which should be made with respect to future experiments.

It would be useful to make a homodyne study using a field of homogeneous turbulence with known rms velocity and known velocity correlation structure. It would then be possible to study the broadening and change of shape (from Lorentzian to Gaussian) of the homodyne spectrum as a function of scattering volume size. Some experiments of this sort have been carried out by Bourke, et al (1969) at Harwell. They were able to compare their homodyne spectra with other data taken using hot wire anemometers and optical heterodyne spectroscopy.

It would be interesting to try to select the wavelength, scattering angle, and type of turbulence so that the Lagrangian scale for the particles in the flow was comparable to the wavelength ($1 / |\vec{K}|$). It would then be possible to obtain information about the joint p.d.f. of particle displacements for two particles as given in equation (37B). As in the previous case, it would greatly aid interpretation of the spectra if the turbulence were homogeneous over the scattering volume.

In experiments with large scattering volumes, it is necessary to keep the rms velocity of the turbulence small so that the spectrum is not broadened so much as to be unobservable. In out experiment, the maximum observable spectrum width using the largest bandwidth available (3 Khz) was judged to be between 50 Khz and 100 Khz, which would be produced by rms turbulent velocities of only .01 to .02 m/s if the scattering volume were large. Larger turbulent velocities could be used if the scattering angle were reduced, if the scattering volume were reduced, or if a more powerful

laser were used.

If the scattering volume is small compared to the turbulent microscale, the width of the spectrum should be determined by the molecular diffusion coefficient. It would be interesting to see experimentally whether or not the turbulence in the fluid has an effect on fluctuations at the molecular level.

When the scattering volume is small, one must be especially careful about two things: 1. The scattering volume should not be made so small that the reciprocal of the particle transit time becomes comparable to the width of the spectrum being observed. 2. It must be verified that the spectrum being observed is not due to fluctuations in the total number of scattering particles in the volume. Repeating the measurement using incoherent light is helpful since observation of the homodyne spectrum requires a highly coherent source.

APPENDIX I

17. Autocorrelation and spectral density of a random process

In this section we collect together some definitions and formulas which concern the autocorrelation and spectral density of a random process. A good discussion at an introductory level about random variables and processes will be found in such books as Davenport and Root (1958) or Papoulis (1965).

In general, a real random process x is a function of time t and a list of random variables which may be written compactly as a multi-dimensional vector $\vec{a}$. In most cases such a process is statistically determined by knowledge of its n^{th}-order distribution function

$$F(x_1, \ldots, x_n; t_1, \ldots t_n) = P[x(t_1) \leq x_1, \ldots, x(t_n) \leq x_n] , \tag{A1}$$

from which one determines by differentiating with respect to all the variables x_i, the n^{th}-order probability density function (p.d.f.)*

$$p(x_1, \ldots, x_n; t_1, \ldots, t_n) dx_1 \ldots dx_n = P[x_1 - dx_1 < x(t_1) \leq x_1, \ldots, x_n - dx_n < x(t_n) \leq x_n] . \tag{A2}$$

The various moments of the random process are then found by multiplying the quantity being averaged by the appropriate p.d.f. and the integrating over the necessary arguments. For example, the mean value of x (which is a function of time for the general, non-stationary process) is given by

$$\overline{x(t)} = \int_{-\infty}^{\infty} dx \; x \, p(x;t) . \tag{A3}$$

The various p.d. functions for the random process x are found by combining and transforming the p.d. functions for the random variables on

---

*For an explanation in detail of the properties of such functions, see Davenport and Root (1958), chapters 2 and 3.

which x depends. In calculating the moments of x, it is often easier to average directly over the random variables $\vec{a}$ instead. For example, the mean value of x would be

$$\bar{x}(t) = \int d\vec{a}\, x(\vec{a}, t) p(\vec{a}), \tag{A4}$$

where f($\vec{a}$) is the joint p.d.f. of the random variables $\vec{a}$. This is the way that averages will be constructed in this paper.

It should be pointed out that in spite of the notation, the various p.d. functions are of course different functions. We shall depend on the context to make it clear which function is required rather than obscure the derivations with unnecessary subscripts or superscripts.

In addition to the mean value, we shall be interested in the autocorrelation of the random process which is in general

$$R_x(t_1, t_2) = \overline{x(t_1)x(t_2)} = \int dx_1 \int dx_2\, x_1 x_2\, p(x_1, x_2; t_1, t_2) = \int d\vec{a}\, x(\vec{a}, t_1) x(\vec{a}, t_2) p(\vec{a}), \tag{A5}$$

where again, the last expression is the one we shall use in making calculations. If a complex process is involved, then one has

$$z(t) = \int d\vec{a}\, z(\vec{a}, t) p(\vec{a}), \tag{A6}$$

and also (the asterisk denotes the complex conjugate)

$$R_z(t_1, t_2) = \overline{z(t_1) z^*(t_2)} = \int d\vec{a}\, z(\vec{a}, t_1) z(\vec{a}, t_2) p(\vec{a}), \tag{A7}$$

from which one has

$$R_z(t_2, t_1) = R_z^*(t_1, t_2). \tag{A8}$$

By averaging over the random variables $\vec{a}$ one avoids having to consider the real and imaginary processes separately.

If the process is stationary, then the autocorrelation function depends only on the time interval $\tau = t_1 - t_2$. Thus we have

$$R_z(\tau) = \overline{z(t+\tau) z^*(t)}, \tag{A9}$$

and also

$$R_z(\tau) = R_z^*(-\tau). \tag{A10}$$

The Fourier transform of the autocorrelation function is the spectral power density function (or simply, power spectrum) $S_z(f)$, where f represents a frequency, $R_z(\tau)$ and $S_z(f)$ are related by

$$S_z(f) = \int_{-\infty}^{\infty} d\tau\, R_z(\tau) \exp(-2\pi i f \tau) , \tag{A11}$$

$$R_z(\tau) = \int_{-\infty}^{\infty} df\, S_z(f) \exp(2\pi i f \tau) . \tag{A12}$$

Using equation (A10), one can easily show that the power spectrum is real. It will be an even function of the argument f when the autocorrelation is real, but otherwise not necessarily. In fact, in the special case where the imaginary part of the complex process z is minus one times the Hilbert transform of the real part process x, then z is known as the analytic signal associated with x and one can show (Papoulis, 1965, p. 357)*

$$S_z(f) = \begin{cases} 2 S_x(f) & f > 0 \\ 0 & f < 0 \end{cases} . \tag{A13}$$

---

*There are unfortunately a multiplicity of ways of defining the set of correlations and transforms associated with the theory of random processes. In this paper we shall follow Bracewell (1965) who defines the Hilbert transform x(t) to be

$$\hat{x}(t) = \frac{1}{\pi} \int_{-\infty}^{\infty} d\tau \frac{x(\tau)}{\tau - t}$$

(the singularity is allowed for by taking the Cauchy principal value) and the analytic signal z(t) to be

$$z(t) = x(t) - i\hat{x}(t)$$

With these definitions, the analytic signal associated with $\cos(a \pm bt)$ is $\exp \pm (a \pm bt)$ where b is taken to be a positive constant. These definitions together with the definitions of the autocorrelation (equation (A9)) and the spectrum (equation (A11)) provide a consistent set of relations such that equation (A13) holds. In optical coherence theory however, it is customary to define the imaginary part of the analytic signal as plus one times the Hilbert transform of the real part and to compensate by using the opposite sign convention in defining the Fourier transform relations, equations (A11) and (A12) (see for example, Beran and Parrent, 1964). With this set of definitions, the analytic signal associated with $\cos(a \pm bt)$ is $\exp \mp (a \pm bt)$. The present author prefers the previous situation in which the frequency b in the exponential always appears with a positive sign, suggesting the fact that the analytic signal contains only positive frequencies.

In the discussion later on, we shall have occasion to use the convolution theorem which, stated briefly, says that the Fourier transform of the product of two quantities is equal to the convolution of their respective Fourier transforms. For example, if

$$R_x(\tau) = R_a(\tau) R_b(\tau) , \tag{A14}$$

and if $S_a(f)$ and $S_b(f)$ are the respective Fourier transforms of $R_a(\tau)$ and $R_b(\tau)$, then the Fourier transforms $S_x(f)$ of $R_x(\tau)$ is given by the convolution integral

$$S_x(f) = \int_{-\infty}^{\infty} df' S_a(f-f') S_b(f') . \tag{A15}$$

A simple extension of this result shows that if

$$R_x(\tau) = R_a(\tau) R_b^*(\tau) , \tag{A16}$$

then

$$S_x(f) = \int_{-\infty}^{\infty} df' S_a(f+f') S_b(f') . \tag{A17}$$

Both of these results may be easily proved by using the Fourier transform equations (A11) and (A12).

Finally, let us write down what we shall consider to be the definition of the Dirac delta function as the Fourier transform of unity,

$$\delta(w-w_0) = \int_{-\infty}^{\infty} dv \exp\left[2\pi i (w-w_0) v\right] . \tag{A18}$$

The most important formula we shall use involving delta functions is the so-called <u>sifting integral</u>

$$\int_{-\infty}^{\infty} dw\, g(w)\, \delta(w-w_0) = g(w_0) . \tag{A19}$$

Other important properties of the Dirac delta function are given in appendix 1 of Davenport and Root (1958).

APPENDIX II

18. The anode photocurrent random process

Studies of shot noise in electronic devices have in the past stimulated the development of the statistical theory of random processes. More recently, attention has been given to the problem of a shot-noise process with a time-varying mean value. This is the type of process which is generated when a photomultiplier is illuminated by light of varying intensity as in the optical homodyne or heterodyne. The autocorrelation and spectral density of the resulting photocurrent in this case are discussed in an appendix to a paper by Freed and Haus (1966). The method used is similar to that used by Davenport and Root (1958) in their discussion of ordinary shot noise. We shall give a brief account of the derivation here for the convenience of the reader. This will also serve to illustrate the method of statistical averaging discussed in section 17.

18.1 Mean Value of the anode photocurrent

We shall assume that the intensity of the scattered light is a stationary random process, and hence that the photocurrent process is also stationary. It is helpful however to consider first the case in which the intensity is not a statistical function at all, but merely a function of time. The photocurrent process in this case is non-stationary. After the required averages have been computed, stationarity is restored by averaging again over the intensity considered statistically.

Let us represent the anode photocurrent as a sum of identical current pulses $i_e(t)$ which occur at random times t_k. We shall neglect the statistical variation in pulse height and shape caused by secondary emission in multiplier tubes. Suppose one considers a photocurrent process

which is non-zero only over an interval of time T during which a random number K of pulses are produced at the anode. If the pulse length is short compared to the length of the interval T, then one may write for this process with negligible error

$$i(T,t) = \begin{cases} \sum_{k=1}^{K} i_e(t-t_k) & -\frac{T}{2} \leq t \leq \frac{T}{2} \\ 0 & \text{otherwise .} \end{cases} \tag{A20}$$

If G is the current gain of the tube and e is the electronic charge, then each current pulse must satisfy the relation

$$\int_{-\infty}^{\infty} dt\, i_e(t) = Ge. \tag{A21}$$

After finding the mean value of the above truncated process, we shall take the limit as T becomes infinitely large; ie.

$$\overline{i(t)} = \lim_{T \to \infty} \overline{i(T,t)}. \tag{A22}$$

The random variables involved here are the K electron emission times and K itself. The statistical average is constructed as in equation (A4)

$$\overline{i(T,t)} = \int dK \int dt_1 \cdots \int dt_K \sum_{k=1}^{K} i_e(t-t_k)\, p(t_1, \cdots, t_K, K) \ . \tag{A23}$$

Interchanging integrations and summation and integrating over variables not involved in the expression being averaged, one has

$$\overline{i(T,t)} = \int dK \sum_{k=1}^{K} dt_k\, i_e(t-t_k)\, p(t_k, K) \ . \tag{A24}$$

Now let us assume that each emission time is independent of the total number of pulses. Then

$$p(t_k, K) = p(t_k \mid K)\, p(K) = p(t_k)\, p(K), \tag{A25}$$

where $p(t_k \mid K)$ is the conditional p.d.f. (Davenport and Root, 1958, p. 29)

Next we assume that the emission time probability for each electron is the same, and that it is proportional to the intensity on the photocathode at any given time. If w(t) represents the light intensity* integrated over the area of the photocathode, then one may write

$$p(t_k) = \begin{cases} \dfrac{w(t_k)}{\int_{-T/2}^{T/2} dt\, w(t)} & -\frac{T}{2} \le t_k \le \frac{T}{2} \\ 0 & \text{otherwise.} \end{cases} \tag{A26}$$

Furthermore, if the emission times of the various electrons are independent, then it has been shown by many authors (for example, Mandel, 1963) that $p(K)$ is a Poisson distribution

$$p(K) = \begin{cases} \dfrac{\bar{k}T}{K!} \exp\left(-\bar{k}T\right) & K = 0, 1, 2, \cdots \\ 0 & \text{otherwise,} \end{cases} \tag{A27}$$

where the emission rate $\bar{k}$ is given by

$$\bar{k}T = \beta \int_{-T/2}^{T/2} dt\, w(t) \quad ; \quad \beta = \frac{\xi\lambda}{hc} \; . \tag{A28}$$

Here ξ is the quanthem efficiency of the photosurface (that is, the mean number of electrons emitted per incident photon), λ is the optical wavelength, h is Planck's constant, and c is the velocity of light. β represents the number of photoelectrons emitted per unit of incident light energy (joules). The above expressions all simplify to the ordinary shot noise expressions in the event that the power w(t) is constant.

Substituting the results of equations (A25) and (A26) into the expression (A24), one finds

$$i(T,t) = \int_{-T/2}^{T/2} dt_k\, i_e(t - t_k) \frac{w(t_k)}{\left[\int_{-T/2}^{T/2} dt\, w(t)\right]} \sum_{K=0}^{\infty} K p(K) \; . \tag{A29}$$

---

*Light intensity has units of power per area, so w(t) has units of power.

But since as can be easily shown

$$\sum_{K=0}^{\infty} K p(K) = \bar{k} T = \beta \int_{-T/2}^{T/2} dt\, w(t) \quad , \tag{A30}$$

the expression for the mean value becomes

$$\overline{i(T,t)} = \beta \int_{-T/2}^{T/2} dt_k\, i_e(t-t_k)\, w(t_k) \, . \tag{A31}$$

Letting T go to infinity and making a change of variable, one has

$$\overline{i(t)} = \beta \int_{-\infty}^{\infty} dt'\, i_e(t')\, w(t-t') \, . \tag{A32}$$

Finally, we assume that w(t) is a stationary random process and average the above expression over the statistics of this process and use equation (A21) to obtain

$$\bar{i} = \beta G_e \bar{w} \quad , \tag{A33}$$

which is the result obtained for the ordinary shot noise process except that the light power is replaced by its mean value.

18.2 Autocorrelation and spectral density of the anode photocurrent

The autocorrelation is calculated with the same procedure used to calculate the mean value. First we consider the intensity to be a simple time function and let the photocurrent be zero except for an interval of time T. The autocorrelation is written as in equation (A5), (we write t for t_1, and $t + \tau$ for t_2),

$$R_i(T,t,\tau) = \int dK \int dt_1 \cdots \int dt_K \sum_{j=1}^{K} \sum_{k=1}^{K} i_e(t-t_j)\, i_e(t-t_k+\tau)\, p(t_1, \ldots t_K, K) \, . \tag{A34}$$

Interchanging integrations and summations and integrating over extraneous variables, one has

$$R_i(T,t,\tau) = \int dK \sum_{j=1}^{K} \sum_{k=1}^{K} \int dt_j \int dt_k \; i_e(t-t_j)\, i_e(t-t_k+\tau)\, p(t_j, t_k, K) \quad . \tag{A35}$$

Next we separate the double sum into the K terms for which j = k and the $(K^2 - K)$ term for which $j \neq k$. Assuming that the random variables t_j, t_k, and K are mutually independent and that the emission time probabilities are the same for each electron, then

$$R_i(T,t,\tau) = \int dK\, p(K) \left[K \int dt_j\, i_e(t-t_j)\, i_e(t-t_j+\tau)\, p(t_j) + (K^2-K) \int dt_j \int dt_k\, i_e(t-t_j)\, i_e(t-t_k+\tau)\, p(t_j)\, p(t_k) \right] . \tag{A36}$$

Since $p(K)$ is given by equation (A27), it can be shown easily that

$$\sum_{K=0}^{\infty} (K^2-K)\, p(K) = (\bar{K}T)^2 = \beta^2 \left[\int_{-T/2}^{T/2} dt\, w(t) \right]^2 . \tag{A37}$$

If $p(t_k)$ is given as before (equation (A26)), then using equations (A30) and (A37), one has

$$R_i(T,t,\tau) = \beta \int_{-T/2}^{T/2} dt_j\, i_e(t-t_j)\, i_e(t-t_j+\tau)\, w(t_j) + \beta^2 \int_{-T/2}^{T/2} dt_j \int_{-T/2}^{T/2} dt_k\, i_e(t-t_j)\, i_e(t-t_k+\tau)\, w(t_j)\, w(t_k) . \tag{A38}$$

Now let T become infinitely large and change the variables around to find

$$R_i(t,\tau) = \beta \int_{-\infty}^{\infty} dt'\, i_e(t')\, i_e(t'+\tau)\, w(t-t') + \beta^2 \int_{-\infty}^{\infty} d\sigma \int_{-\infty}^{\infty} dt'\, i_e(t')\, i_e(\sigma+t')\, w(t-t')\, w(t-t'+\tau-\sigma) . \tag{A39}$$

The final step is to consider w(t) a stationary random process and to carry out an average with respect to this process. If we let

$$R_0(\tau) = \int dt'\, i_e(t')\, i_e(t'+\tau) \quad , \tag{A40}$$

then

$$R_i(\tau) = \beta \bar{w} R_o(\tau) + \beta^2 \int_{-\infty}^{\infty} d\sigma R_o(\sigma) R_w(\tau - \sigma) , \tag{A41}$$

which is the result given by Freed and Haus (1966) when all the current pulses are assumed to be of the same shape. If the light intensity is a constant, this result reduces to equation (7-36) of Davenport and Root (1958).

It is usually the case in the homodyne experiment that the intensity fluctuation is small over a time as short as the current pulse length. Mathematically, this situation can be approximated by assuming the current pulses to be delta-functions such as

$$i_e(t) = Ge\,\delta(t) , \tag{A42}$$

in which case

$$R_o(\tau) = (Ge)^2 \delta(\tau) . \tag{A43}$$

Equation (A41) becomes

$$R_i(\tau) = Ge\,\bar{i}\,\delta(\tau) + \left(\frac{\bar{i}}{\bar{w}}\right)^2 R_w(\tau) \quad ; \quad \bar{i} = \beta Ge\,\bar{w} . \tag{A44}$$

The spectral intensity of the anode photocurrent is defined for our purpose by equation (A11). The general expression obtained by Fourier transforming equation (A41) (making use of the convolution theorem, equations (A14) and (A15)) is

$$S_i(f) = \beta \bar{w} S_o(f) + \beta^2 S_o(f) S_w(f) , \tag{A45}$$

where $S_o(f)$ and $S_w(f)$ are the Fourier transforms of $R_o(\tau)$ and $R_w(\tau)$. When the intensity varies only slowly over the duration of a pulse, an approximation to the spectrum valid at low frequencies is found by transforming equation (A44)

$$S_i(f) = Ge\,\bar{i} + \left(\frac{\bar{i}}{\bar{w}}\right)^2 S_w(f) . \tag{A46}$$

Thus the photocurrent spectral density consists of two parts: the shot-noise part which is frequency independent at low frequencies, and the optical fluctuation part which at low frequencies is simply proportioned to the spectrum of the light power.

If it is now assumed that the photocathode is coherently illuminated so that

$$w(t) = A\, I(t) \ ,$$

where A is the cathode area and I(t) is the intensity of the light, then equation (A46) becomes

$$S_i(f) = Ge\bar{i} + \left(\frac{\bar{i}}{\bar{I}}\right)^2 S_I(f) \ . \qquad \text{(A47)}$$

This result is given in the text as equation (1).

APPENDIX III

19. The scattered electric field

Expressions for the radiation fields of an infinitesimal electric dipole can be found in Born and Wolf (1965). Using these results, we shall obtain an expression for the scattered electric field when a collection of point dipoles is illuminated by a plane electromagnetic wave. Attenuation of the wave and multiple scattering are neglected. The dipoles may move about, but their velocities must be small compared to the velocity of light.

A particular solution of Maxwell's equations for the electric field $\vec{E}$ as a function of position $\vec{\rho}$ and time t is given by Born and Wolf, (1965; p. 80): *

$$\vec{E}(\vec{\rho},t) = \left\{\frac{1}{4\pi\epsilon_0}\right\}\left(-\frac{1}{c^2}\frac{\partial^2}{\partial t^2} + \text{grad div}\right)\int_{\text{ALL SPACE}} d\vec{\pi}\,\frac{\vec{P}\left(\vec{\pi}, t-\frac{R}{c}\right)}{R}, \qquad \text{(B1)}$$

where

$$R = |\vec{\pi} - \vec{\rho}|, \qquad \text{(B2)}$$

$\vec{P}$ is the polarization field induced by the incident radiation, ϵ_0 is the free space permittivity, and the space derivatives are with respect to the field point $\vec{\rho}$. If the illuminated dipoles are confined to some fixed finite region, and if the electric field is to be evaluated at a point outside this region, then the integration does not involve a singularity and the derivatives may be taken inside the integral. One may carry out the indicated differentiation as Born and Wolf have done for a single point

*Equations are given in rationalized MKS form. To obtain Gaussian cgs equations, omit the factor in braces.

dipole. In the radiation zone one obtains

$$E(\vec{\Delta},t) \simeq \left\{\frac{1}{4\pi\epsilon_0}\right\} \frac{\sin\Upsilon}{c^2} \int d\vec{\pi}\, \frac{1}{R}\, \frac{\partial^2}{\partial t^2}\, P\left|\vec{\pi}, t - \frac{R}{c}\right| , \tag{B3}$$

where Υ is angle between the incident electric field and the direction of the scattering.

The polarization field is found by summing the polarization fields produced at the individual dipoles. The polarization induced in the $j^{\underline{th}}$ dipole located at $\vec{\pi}_j(t)$ is assumed to be proportional to the incident electric field $\vec{E}(\vec{r},t)$ and a constant, scalar polarizability α. The polarization field is then written as a sum of δ-functions

$$P(\vec{\pi},t) = \{4\pi\epsilon_0\}\, \alpha\, \vec{E}(\vec{\pi},t) \sum_{j=1}^{N} \delta\left[\vec{\pi} - \vec{\pi}_j(t)\right] , \tag{B4}$$

where N is the total number of dipoles.

Although the electric fields and polarization fields are real quantities, we shall find it more convenient to deal with the associated analytic signals (see Appendix I, particularly the note on p. 73) In particular, let us assume that the incident electric field is a plane wave of the form

$$\vec{E}(\vec{\pi},t) = \vec{E}_0 \exp i\left|\omega_0 t - \vec{k}_0 \cdot \vec{\pi}\right| , \tag{B5}$$

where

$$\left|\vec{k}_0\right| = \frac{\omega_0}{c} , \tag{B6}$$

and $\omega_0 = 2\pi f_0$ is a real, constant angular frequency.

The dipoles are assumed to move with velocities that are small compared to the velocity of light. In taking the time derivatives required in equation (4), we neglect the slow variation in $\vec{P}$ due to particle motion compared with the rapid oscillations of the incident field and write

$$\frac{\partial^2}{\partial t^2}\, P(\vec{\pi},t) \simeq -\omega_0^2\, P(\vec{\pi},t) \quad ; \tag{B7}$$

also

$$\vec{r}_j\left(t-\frac{R}{c}\right) \simeq \vec{r}_j(t) \,. \tag{B8}$$

Substituting into equation (4), we find

$$\vec{E}(\vec{s},t) \simeq -q_0 \sum_{j=1}^{N} \frac{1}{R_j} \exp i\left[\omega_0\left|t-\frac{R_j}{c}\right| - k_0 \cdot \vec{r}_j(t)\right] , \tag{B9}$$

where

$$q_0 = \alpha k_0^2 E_0 \sin\gamma . \tag{B10}$$

The geometry associated with the scattering region is shown in Fig. 1. Let $\vec{k}_s$ be the wave vector in the scattering direction and note that $|\vec{k}_s| \simeq |\vec{k}_0|$. If the distance to the field point is large compared with the dimensions of the scattering volume, then approximately

$$R_j \simeq s - \frac{\vec{k}_s \cdot \vec{r}_j}{k_s} , \tag{B11}$$

and

$$\frac{1}{R_j} \simeq \frac{1}{s} . \tag{B12}$$

We define a difference wave vector $\vec{K}$

$$\vec{K} = \vec{k}_0 - \vec{k}_s , \tag{B13}$$

and note incidentally that

$$|\vec{K}| = \frac{4\pi}{\lambda_0} \sin\frac{\theta}{2} , \tag{B14}$$

where λ_0 is the optical wavelength (c/f_0) and θ is the angle between the incident and scattered wave vectors. Upon substituting these geometrical approximations into equation (9) we find

$$\vec{E}(\vec{s},t) \simeq -\frac{q_0}{s} \exp i\left|\omega_0 t - k_0 s\right| \sum_{j=1}^{N} \exp\left[-i\vec{K}\cdot\vec{r}_j(t)\right] . \tag{B15}$$

This is the expression we require for the scattered electric field and which appears as equation (7) in the text.

APPENDIX IV

20. Space-time correlation of the scattered intensity and the area of coherence

In Chapter II it was indicated that fluctuations in the scattered light intensity produce fluctuations in the photocurrent which are spectrally analyzed in the optical homodyne. The discussion was restricted to the case in which the cathode was coherently illuminated. In this section, we consider the more general case and show that the coherence area for scattering from a random collection of particles is given approximately by λ^2/Θ, where Θ is the solid angle subtended by the scattering volume at the cathode. The results of this section and the one to follow further show that the signal-to-noise ratio for the optical homodyne is independent of the number of coherence areas seen by the cathode, as long as there is at least one.

The basic concepts discussed in this section were outlined qualitatively by Forrester, Gudmundsen, and Johnson (1955) and by Forrester (1961). Their results as applied to a homodyne experiment were confirmed recently by Berge, Volochine, Calmettes, and Hamelin (1968).

We will assume that the scattering particle statistics are stationary in time and homogeneous in space, and that the particles are located and move independently. The results are compared with an expression given by Berge, et al.

The spectrum of the homodyne photocurrent was given in terms of the spectrum of the scattered light power w(t) by equation (A46) above. The light power is, by definition, the integral of the scattered intensity $I(\vec{s},t)$ over the photocathode area A, that is,

$$w(t) = \int_A \vec{ds}\ I(\vec{s}, t). \tag{A48}$$

The autocorrelation of the light power is thus

$$R_w(\tau) = \int_A \vec{ds}_1 \int_A \vec{ds}_2\ R_I(\vec{s}_1, \vec{s}_2; \tau), \tag{A49}$$

where

$$R_I(\vec{s}_1, \vec{s}_2; \tau) = \overline{I(\vec{s}_1, t_1)\, I(\vec{s}_2, t_2)}. \tag{A50}$$

If the intensity fluctuations occur simultaneously over the entire photocathode, the cathode is said to be coherently illuminated, and

$$R_w(\tau) = A^2 R_I(\tau). \tag{A51}$$

In general, however, one must consider the complete space-time correlation indicated in equation (A50).

As in Chapter II, it is easier to consider first the space-time correlation for the electric field $R_E(\vec{s}_1, \vec{s}_2; \tau)$. Starting with the electric field as given in equation (7) (~~we neglect motion of particles through the volume~~), and following the procedure which led to equation (16), we find the result

$$R_E(\vec{\rho}_1, \vec{\rho}_2; \tau) = \frac{Nq_0^2}{\Delta^2} \exp i[\omega_0 \tau - k_0 \Delta] \int d\vec{\pi}_1 \int d\vec{\pi}_2 \exp i[\vec{K}_2 \cdot \vec{\pi}_2 - \vec{K}_1 \cdot \vec{\pi}_1]\, p(\vec{\pi}_1, \vec{\pi}_2; \tau), \tag{A52}$$

where

$$\sigma = |\vec{\sigma}| = |\vec{\rho}_1 - \vec{\rho}_2|,$$

$$\vec{K}_1 = \vec{k}_0 - \vec{k}_{s1}, \tag{A53}$$

$$\vec{K}_2 = \vec{k}_o - \vec{k}_{s2},$$

and $\vec{k}_{s1}$ and $\vec{k}_{s2}$ are wave vectors pointing in the $\vec{s}_1$ and $\vec{s}_2$ direction, respectively. Let

$$\vec{\Delta K} = \vec{K}_1 - \vec{K}_2 = \vec{k}_{s2} - \vec{k}_{s1} \tag{A54}$$

and eliminate $\vec{K}_2$ from equation (A52) to obtain

$$R_E(\vec{\rho}_1, \vec{\rho}_2; \tau) = \frac{q_o^2 N}{A^2} \exp i[\omega_o \tau - k_o \sigma] \int d\vec{\pi}_1 \int d\vec{\pi}_2 \exp i \vec{K}_1 \cdot (\vec{\pi}_2 - \vec{\pi}_1) \times \exp[-i \vec{\Delta K} \cdot \vec{\pi}_2] \, p(\vec{\pi}_1, \vec{\pi}_2; \tau) \tag{A55}$$

Note that $\vec{\Delta K}$ is a function of $\vec{s}_1$ and $\vec{s}_2$. If the particle statistics are homogeneous, then equation (17) holds and one has

$$R_E(\vec{\rho}_1, \vec{\rho}_2; \tau) = R_E(\tau) \exp[-ik_o \sigma] \frac{1}{V} \int_V d\vec{\pi} \exp[-i \vec{\Delta K} \cdot \vec{\pi}] \tag{A56}$$

where $R_E(\tau)$ is given by equation (18). Equation (A56) is an interesting result in that it shows that the space-time correlation can in this case be factored into the product of the time correlation at a single point and the space correlation at a single time. This property is referred to as cross-spectral purity (Mandel, 1963) and is seen to depend on the assumption of homogeneity.

The space-time intensity correlation is found by starting with equation (12) for the intensity and by following the procedure which led to equation (34). When it is assumed that the particle motions are independent so that equation (35) holds, then one obtains

$$R_I(\vec{\rho}_1, \vec{\rho}_2; \tau) = I(\vec{\rho}_1) I(\vec{\rho}_2) + C^2 R_E(\vec{\rho}_1, \vec{\rho}_2; \tau) R_E^*(\vec{\rho}_1, \vec{\rho}_2; \tau) \tag{A57}$$

which is the generalization of equation (36).

Let us evaluate the integral in equation (A56) when the scattering is observed at an angle of 90^{o} from a segment of laser beam of length a and diameter b. It is possible to perform the calculation by integrating over the cylindrical volume thus defined, but it is easier to ignore the thickness of the beam in the scattering direction and to replace the volume integral by a two dimensional integral over a rectangle of length a and height b (see Fig. 17). The two results differ only by a numerical factor.

The vector $\vec{\Delta K}$ is easily shown to lie in the plane of integration normal to the scattering direction, and to be of magnitude $k_o \sigma / s$, where $\vec{\sigma}$ was defined in equation (A53) and lies in the plane of the cathode. One can write

$$\vec{\Delta K} \cdot \vec{\pi} = \frac{k_o}{s} \left| \sigma_x \pi_x + \sigma_y \pi_y \right| , \tag{A58}$$

where x and y designate components of the vectors in the plane perpendicular to the scattering direction, with the dimension a along x and the dimension b along y. The integration yields

$$\frac{1}{ab} \int_{-a/2}^{a/2} d\pi_x \int_{-b/2}^{b/2} d\pi_y \exp -i \frac{k_o}{s} \sigma_x \pi_x + \sigma_y \pi_y = \left\{ \frac{\sin \frac{k_o \sigma_x a}{2s}}{\frac{k_o \sigma_x a}{2s}} \right\} \left\{ \frac{\sin \frac{k_o \sigma_y b}{2s}}{\frac{k_o \sigma_y b}{2s}} \right\} , \tag{A59}$$

which is the diffraction pattern of a rectangular aperture. The identification of the spatial correlation function of an incoherent, plane source with the diffraction pattern of an aperture having the same shape as that source is the substance of the van Cittert-Zernike theorem of the theory of partial coherence (see Born and Wolf, 1965, p. 508).

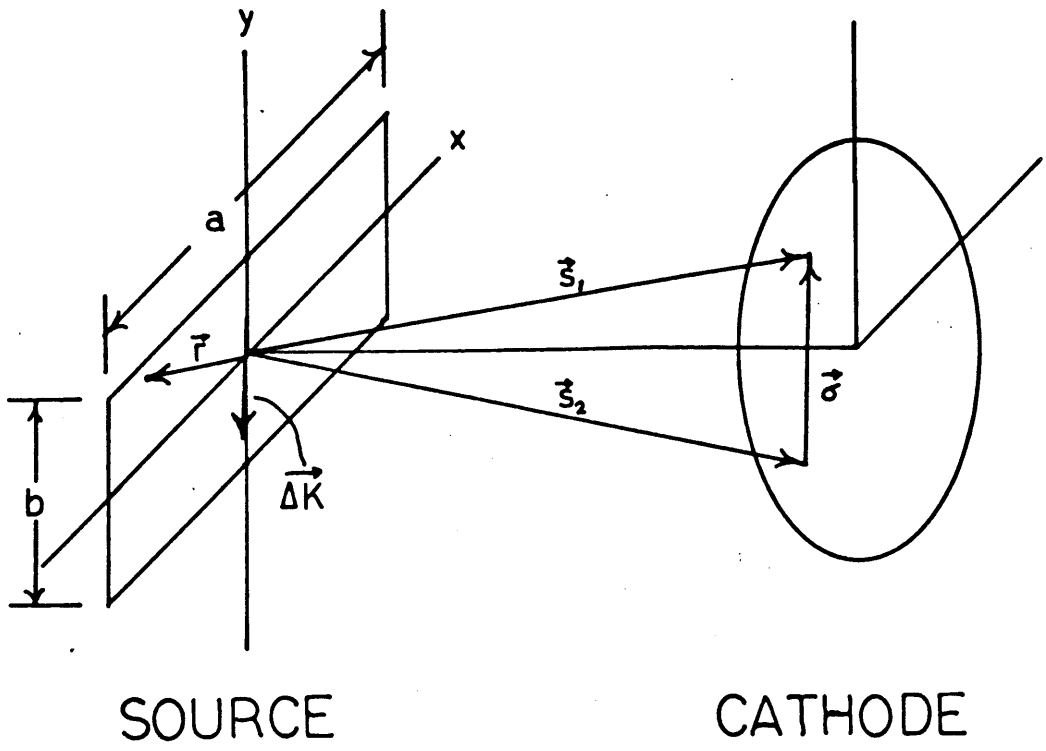

Fig. 17. Geometry of the spatial correlation calculation.

Equation (A56) now reads

$$R_E(\vec{\sigma};\tau) = R_E(\tau)\exp(-ik_0\sigma)\left\{\frac{\sin\frac{k_0\sigma_x a}{2s}}{\frac{k_0\sigma_x a}{2s}}\right\}\left\{\frac{\sin\frac{k_0\sigma_y b}{2s}}{\frac{k_0\sigma_y b}{2s}}\right\} , \tag{A60}$$

so that the intensity correlation (equation (A49)) can be written

$$R_I(\vec{\sigma};\tau) = \bar{I}^2 + C^2 R_E(\tau)R_E^*(\tau)\left\{\frac{\sin\frac{k_0\sigma_x a}{2s}}{\frac{k_0\sigma_x a}{2s}}\right\}^2\left\{\frac{\sin\frac{k_0\sigma_y b}{2s}}{\frac{k_0\sigma_y b}{2s}}\right\}^2 . \tag{A61}$$

If the area of coherence is taken to be the rectangular area on the cathode bounded by the first zeros of the two sine functions, then it is found that

$$A_{coh} = \frac{\lambda^2}{\Theta} , \tag{A62}$$

where

$$\Theta = \frac{ab}{s^2} . \tag{A63}$$

Θ is the solid angle subtended by the source as seen from the cathode. Equation (A62) is approximately true regardless of the shape of the source volume, as long as the scattering particles have homogeneous statistics and are located and move independently.

Let us now substitute equation (A61) into equation (A49) and obtain an expression for $R_w(\tau)$. We assume that the coherence area is small compared to the cathode area so that the integration over $\vec{s}_1$ may be replaced by integration over $\vec{\sigma}$ with limits extended to infinity. The integration over $\vec{s}_2$ gives the area A. We have

$$R_w(\tau) = \bar{I}^2A^2 + e^2R_E(\tau)R_E^*(\tau)A\int_{-\infty}^{\infty}d\sigma_x\left\{\frac{\sin\frac{k_0\sigma_x a}{2\delta}}{\frac{k_0\sigma_x a}{2\delta}}\right\}^2\int_{-\infty}^{\infty}d\sigma_y\left\{\frac{\sin\frac{k_0\sigma_y b}{2\delta}}{\frac{k_0\sigma_y b}{2\delta}}\right\}^2$$

$$= \bar{I}^2A^2\left[1 + \frac{A_{coh}}{A}\frac{e^2R_E(\tau)R_E^*(\tau)}{\bar{I}^2}\right] . \qquad \text{(A64)}$$

The final step in this development is to Fourier transform equation (A64), and substitute the result into equation (A46) for $S_i(f)$ (note that $\bar{w} = \bar{I}A$) to obtain

$$S_i(f) = \bar{i}^2\delta(f) + Ge\bar{i} + \left(\frac{\bar{i}}{\bar{I}}\right)^2\frac{A_{coh}}{A}e^2\int_{-\infty}^{\infty}df'S_E(f+f')S_E(f') . \qquad \text{(A65)}$$

Apart from the zero-frequency impulse, the anode photocurrent spectrum is seen to consist of a shot-noise part and an optical fluctuation part. Moreover, since the mean photocurrent for a given mean incident intensity is proportional to the cathode area A, one can see from equation (A65) that increasing the area of the cathode causes the shot-noise part and the fluctuation part to increase proportionally. As we shall see in the next section, the signal-to-noise ratio for the experiment is independent of the cathode area utilized, so long as it includes at least one coherence area.

A comparison with the experimental study of Berge, et al (1968) is easily obtained from equation (A65). Suppose that the electric field spectrum ~~f_0 HWHM~~ is Lorentzian with a HWHM of f_0 hz, and then ask how much power from the fluctuation part of the spectrum passes through a frequency band from - Δf to + Δf where Δf is small compared to f_0. The result is

$$\overline{i_F^2(f)}\Big|_{f=0} = \frac{1}{\pi}\bar{i}^2\frac{\Delta f}{f}\frac{A_{coh}}{A} , \qquad \text{(A66)}$$

which is equation (1) of Berge, et al. They measured $\overline{i_F^2(f)}$ in a homodyne experiment as a function of A_{coh} and A and found good agreement with this result.

APPENDIX V

21. Signal-to-noise ratio for the homodyne spectrometer

In this section we give a few results concerning the observability of the homodyne spectrum that may be of interest to someone planning an experiment. An expression for the signal-to-noise ratio is given and discussed, though an explicit derivation is not provided.

Let us first of all compare the magnitude of the power in the fluctuation part of the spectrum with the magnitude of the power in the shot-noise part (see equation (A65)). Equation (A66) gave the amount of power in the fluctuation part of the spectrum which passes through a frequency band extending from $-\Delta f$ to $+\Delta f$ where Δf is small compared to the width f_o of a Lorentzian electric-field spectrum. The analogous result for the shot-noise power is

$$\overline{i_N^2(f)} = 2\,Ge\,\bar{i}\,\Delta f. \tag{A67}$$

Forming the ratio and recalling that equation (A33)

$$\bar{i} = BGe\,\bar{w} = BGe\,A\bar{I}, \tag{A68}$$

one has

$$\left.\frac{\overline{i_F^2(f)}}{\overline{i_N^2(f)}}\right|_{f=0} = \beta\bar{I}\frac{A_{coh}}{2\pi f_o} \equiv \zeta\delta\,, \tag{A69}$$

where ζ is the quantum efficiency as introduced in equation (A28) and δ is the degeneracy parameter for the incident light. δ represents the number of photons incident on a coherence area of the cathode in a coherence time. The ratio in equation (A69) is thus equal to the number of photo-electrons emitted by a single coherence area in a coherence time. Mixing experiments using incoherent light such as the one performed by Forrester,

Gudmundsen, and Johnson (1955) are generally very difficult because the degeneracy parameter for such sources is usually very small. Note that increasing the cathode area has no effect on the fundamental ratio in equation (A69).

The signal in the experiment may be taken to be the power in the fluctuation part of the spectrum $\overline{i_F^2}(f)$. The noise in the experiment should be taken to be the experimental uncertainty in determining this quantity. Detection of the homodyne spectrum is accomplished by passing the photocurrent through a narrowband filter of width Δf_1, a square-law device, and a low pass filter of width Δf_2. The signal-to-noise ratio for such a process can be shown to be given by

$$\left.\frac{S}{N}\right|_{f=0} = \frac{\S\delta}{1+\S\delta}\sqrt{\frac{1}{2}\frac{\Delta f_1}{\Delta f_2}} \qquad \text{(A70)}$$

Thus, even though $\S\delta$ may be small compared to unity, the experiment may still be made possible by making the ratio $\Delta f_1/\ \Delta f_2$ large enough. This is equivalent to using a longer integration time in observing the output.

LIST OF SYMBOLS

Symbol	Meaning	Page
$\vec{a}$	multi-dimensional vector representing a list of random variables	71
a	radius of spherical volume; particle radius	32
a,b	dimensions	89
A	area of photocathode	86
B	friction constant	32
c	velocity of light	
$\mathcal{C}$	specified constant	22
d	nozzle diameter	60
D	diffusion coefficient	27;32
e	electronic charge	
$\vec{E}(\vec{r},t)$	complex electric field	19
f; f_o	frequency; incident laser frequency; ~~probability density function~~	21
G	photomultiplier current gain	76
h	Planck's constant	
i	$\sqrt{-1}$	
i(t)	photocurrent	76
$i_e(t)$	shape of elementary current pulse	75
$I(\vec{r},t)$	light intensity (power/area)	22
$\bar{k}$	mean rate at which photoelectrons are emitted	77
$\vec{k}$; $\vec{k}_o$; $\vec{k}_s$	wave vector; incident wave vector; scattered wave vector	19

Symbol	Meaning	Page
k_B	Boltzmann constant	
K	number of photoelectrons emitted in an interval	76
$\vec{K}$	$\vec{k}_o - \vec{k}_s$	21
$\vec{\Delta K}$	$\vec{K}_1 - \vec{K}_2$	88
m	mass of particle	32
N	total number of dipoles	21
p(x)	probability density function	71
$\vec{P}(\vec{r}, t)$	polarizability field	82
q_o	specified constant	21
$\vec{r}$; $\vec{s}$	position vectors (source point; field point)	20
$\vec{r}_j(t)$	location of j^{th} particle at time t	20
$\vec{r}_1$	location of particle at time t_1, etc.	23
$\vec{r}_{12}$	location of particle 1 at time 2, etc.	29
$R_a(\tau)$	autocorrelation of random process a(t)	72
Re	Reynolds number	40
$S_a(f)$	power density spectrum of random process a(t)	73
t	time	
T	particle transit time	47
$\vec{v}(\vec{r}, t)$	velocity	36
V_o	nozzle velocity	60
V	scattering volume	23
w(t)	light power	76
z; z_o	axial distance from nozzle; location of geometrical origin	60

Symbol	Meaning	Page
α	polarizability	83
$\alpha(\vec{\Delta})$	velocity correlation function	37
β	specified constant	77
γ	angle between incident electric field and scattering direction	21
δ	degeneracy of parameter	94
$\delta(f)$	Dirac delta-function	74
ϵ_o	permittivity of free space	
η	viscosity	32
θ	scattering angle	20
Θ	solid angle	91
λ	wavelength	21
Λ; L	integral scale (Lagrangian; Eulerian)	32;59
μ_o	permeability of free space	
ν	kinematic viscosity	40
ξ	quantum efficiency	77
$\vec{\rho}$; $\vec{\sigma}$; $\vec{\Delta}$	space intervals	24;87;30
τ	time interval	
ω; ω_o	angular frequency; incident angular frequency	19

BIBLIOGRAPHY

Abramovich, G. N., The Theory of Turbulent Jets, trans. by Scripta Technica, Cambridge, Mass.: M.I.T. Press, 1963.

Alpert, S. S., Time dependent concentration fluctuations near the critical temperature, in Conf. on Phenomena in the Neighborhood of Critical Points, U.S.N.B.S., Misc. Publ. 273, 1966.

Alpert, S. S., Y. Yeh, and E. Lipworth, Observation of time dependent concentration fluctuations in a binary mixture near the critical temperature using a He-Ne laser, Phys. Rev. Letters, 14:486-8, (1965).

Arecchi, F. T., M. Giglio, and U. Tartari, Scattering of coherent light by a statistical medium, Phys. Rev., 163:186-94, (1967).

Aref'ev, I. M., B. D. Kopylovskii, D. Sh. Mash, and I. L. Fabelinskii, Determination of diffusion coefficients by heterodyning light scattered by liquid solutions, Soviet Physics, J.E.T.P. Letters, 5:355-8, (1967).

Batchelor, G. K., The Theory of Homogeneous Turbulence, Cambridge, England: Cambridge Univ. Press, 1953.

Becker, H. A., Concentration Fluctuations in Ducted Jet-Mixing, Ph.D. thesis, Dept. of Chem. Eng., M.I.T., Cambridge, Mass., 1961.

Becker, H. A., H. C. Hottel, and G. C. Williams, On the light-scatter technique for the study of turbulence and mixing, J. Fluid Mech., 30:259-84, (1967).

Beran, M. J., and G. B. Parrent, Jr., Theory of Partial Coherence, Englewood Cliffs, N.J.: Prentice-Hall, Inc., 1964.

Berge, P., B. Volochine, P. Calmettes, and A. Hamelin, Influence de la coherence spatiale de la lumière sur l'intensite des signaux de battements de photons, Compt. Rend. Acad. Sci., 266:1575-8, (1968).

Born, M., and E. Wolf, Principles of Optics, 3rd. ed., New York: Pergamon Press, 1965.

Bourke, P. J., L. E. Drain, P. Hutchinson, D. A. Jackson, B. Moss, E. R. Pike, and P. Shofield, Observation of spatial correlation of turbulent velocity by laser anemometry, preprint, Chemical Engineering Division, A.E.R.E., Harwell, England, 1969.

Bracewell, R., The Fourier Transform and its Applications, New York: McGraw-Hill Book Co., 1965.

Chandrasekhar, S., Stochastic problems in physics and astronomy, Rev. Mod. Phys., 15:1-89, (1943). Reprinted as pp. 3-91 of N. Wax, ed., Selected Papers on Noise and Stochastic Processes, New York: Dover, 1954.

Cummins, H. Z., N. Knable, and Y. Yeh, Observation of diffusion broadening of Rayleigh scattered light, Phys. Rev. Letters, 12: 150-3, (1964).

Davenport, W. B., Jr., and W. L. Root, An Introduction to the Theory of Random Signals and Noise, New York: McGraw-Hill Book Co., Inc., 1958.

Dubin, S. B., J. H. Lunacek, and G. B. Benedek, Observation of the spectrum of light scattered by solutions of biological macromolecules, Nat. Acad. Sci. Proc., 57:1164-71, (1967).

Dunning, J. W., and J. C. Angus, Particle-size measurement by Doppler-shifted laser light, a test of the Stokes-Einstein relation, J. Appl. Phys., 39:2479-80, (1968).

Fiocco, G., and J. B. DeWolf, Frequency spectrum of laser echoes from atmospheric constituents and determination of the aerosol content of air, J. Atmos. Sci., 25:488-96, (1968).

Fleisher, A., Information contained in weather noise, M.I.T. Dept. of Meteorol., Weather Radar Res. Tech. Rep. No. 22A, 42 pp, 1953.

Ford, N. C., Jr., and G. B. Benedek, Observations of the spectrum of light scattered from a pure fluid near its critical point, Phys. Rev. Letters, 15:649-53, (1965).

Ford, N. C., Jr., and G. B. Benedek, The spectrum of light inelastically scattered by a fluid near its critical point, in Conf. on Phenomena in the Neighborhood of Critical Points, N.B.S., Misc. Publ. 273, 1966.

Forrester, A. T., Photoelectric mixing as a spectroscopic tool, J. Opt. Soc. Am., 51:253-9, (1961).

Forrester, A. T., R. A. Gudmundsen, and P. O. Johnson, Photoelectric mixing of incoherent light, Phys. Rev., 99:1691-1700, (1955).

Freed, C., and H. A. Haus, Photoelectric spectrum and photoelectron counts produced by a gaseous laser, Phys. Rev., 141:287-98, (1966).

Frenkiel, F., and P. Kelbanoff, Higher-order correlations in a turbulent field, Phys. Fluids, 10:507-20, (1967).

Frisch, H., Study of turbulence by spectral fine structure of scattered light, Phys. Rev. Letters, 19:1278-9, (1967).

Goldstein, R. J., and W. F. Hagen, Turbulent flow measurents utilizing the Doppler shift of scattered laser radiation, Phys. Fluids, 10: 1349-52, (1967).

Goldstein, R. J., and D. K. Kreid, Measurement of laminar flow development in a square duct using a laser-Doppler flowmeter, J. Appl. Mech., 34:813-8, (1967).

Hinze, J. O., Turbulence, New York: McGraw-Hill Book Co., 1959.

Hulst, H. C. van de, Light scattering by Small Particles, New York: Wiley, 1957.

Komarov, L. I., and I. Z. Fisher, Theory of Rayleigh scattering of light in liquids, Soviet Phys. J.E.T.P., 16:1358-61, (1963).

Lastovka, J. B., and G. B. Benedek, Light-beating techniques for the study of the Rayleigh-Brillouin spectrum, in P. L. Kelley, B. Lax, and P. C. Tannenwald, eds., Physics of Quantum Electronics, New York: McGraw-Hill Book Co., 1966A.

Lastovka, J. B., and G. B. Benedek, Spectrum of light scattered quasielastically from a normal liquid, Phys. Rev. Letters, 17: 1039-42, (1966B).

Lawson, J. L., and G. E. Uhlenbeck, Threshold Signals, New York: Dover, 1950.

Mandel, L., Fluctuations in light beams, in E. Wolf, ed., Progress in Optics, vol. 2, New York: Intersciences, 1963.

McIntyre, D., and F. Gornick, eds., Light Scattering from Dilute Polymer Solutions, New York: Gordon and Breach, 1964.

Papoulis, A., Probability, Random Variables, and Stochastic Processes, New York: McGraw-Hill Book Co., 1965.

Pecora, R., Doppler shifts in light scattering from pure liquids and polymer solutions, J. Chem. Phys., 40:1604-14, (1964).

Pike, E. R., D. A. Jackson, P. J. Bourke, D. I. Page, Measurement of turbulent velocities from the Doppler shift in scattered laser light, J. Sci. Instrum., 1:727-30, (1968).

Reynolds, A. J., Observations of a liquid-into-liquid jet, J. Fluid Mech., 14:552-6, (1962).

Rosler, R. S., and S. G. Bankoff, Large-scale turbulence characteristics of a submerged water jet, A. I. Ch. E. Journal, 9:672-6, (1963).

Smith, A. W., and G. W. Williams, On the detection of maser signals by photoelectric mixing, J. Opt. Soc. Am., 52:337-8, (1962).

Van Hove, L., Correlations in space and time and Born approximation scattering in systems of interacting particles, Phys. Rev., 95: 249-62, (1954).

White, D. A., Velocity measurements in axisymmetric jet of dilute polymer solutions, J. Fluid Mech., 28:195-204, (1967).

White, J. A., J. S. Osmundson, and B. H. Ahn, Onset of long-range order in a critical solution of macromolecules, Phys. Rev. Letters, 16: 639-42, (1962).

BIOGRAPHICAL NOTE

The author was born on July 26, 1942, in Salem, Massachusetts. He lived in Swampscott, Massachusetts for ten years, then moved with his family to Erie, Pennsylvania where he graduated from Academy High School in June of 1960. He attended Princeton University from September, 1960 until June, 1964, when he received an A.B. degree in physics. His senior thesis at Princeton concerned the measurement of the angular size of stellar images during the day. During the summers of 1963 and 1964 he was employed as a research assistant on a seismic crustal studies program in the Lake Superior region. In September, 1964, he enrolled as a graduate student at M. I. T. in the Department of Geology and Geophysics (now, Earth and Planetary Sciences). He received an S.M. degree in February, 1967, and his Master's thesis was titled, "On the Measurement of Atmospheric Temperature by Optical Radar". His thesis advisor was Dr. Giorgio Fiocco. In 1968, with Dr. Fiocco he published a paper concerning light scattering from atmospheric constituents (Fiocco and DeWolf, 1968). The author's other interests include music and mountaineering.